Palaeogeography, Palaeoclimatology, Palaeoecology, 96 (1992): 233–260
Elsevier Science Publishers B.V., Amsterdam

Stable isotope and foraminiferal changes across the Cretaceous–Tertiary boundary at Stevns Klint, Denmark: Arguments for long-term oceanic instability before and after bolide-impact event

Birger Schmitz[a], Gerta Keller[b] and Olof Stenvall[a]

[a] *Department of Marine Geology, Box 7064, University of Gothenburg, S-402 32 Gothenburg, Sweden*
[b] *Department of Geological and Geophysical Sciences, Princeton University, Princeton, NJ 08544, USA*

(Received August 29, 1991; revised and accepted May 14, 1992)

ABSTRACT

Schmitz, B., Keller, G. and Stenvall, O., 1992. Stable isotope and foraminiferal changes across the Cretaceous–Tertiary boundary at Stevns Klint, Denmark: Arguments for long-term oceanic instability before and after bolide-impact event. Palaeogeogr., Palaeoclimatol., Palaeoecol., 96: 233–260.

Stable isotope and planktic and benthic foraminiferal analyses of the K/T boundary transition at Stevns Klint, Denmark, indicate a 100–500 kyr long period of instability in oceanic bottom-water temperature and sea level. During the latest Maastrichtian (from 2.7 m below and up to the K/T boundary) bottom-water temperatures gradually cooled about 1.5°C as surface water temperatures remained constant. At the K/T boundary bottom water temperatures decreased additionally 3°C, and then returned to pre-boundary values just above the boundary interval. Coincident with the onset of the first temperature decrease there was a prominent sea-level fall, estimated between 50–100 m as observed in benthic and planktic foraminiferal assemblages as well as in a decreasing surface-to-bottom $\delta^{13}C$ gradient. About 40 cm below the iridium-rich K/T boundary clay, sea level began to rise. Poor preservation of foraminifera above the K/T boundary allows only tentative interpretation of Danian events at Stevns Klint, however, sea level generally continued to rise interrupted by short sea level falls. Associated with the observed sea-level changes are three important hiatuses: At the contact between the white chalk and overlying grey-white bryozoan chalk about 2.7 m below the K/T boundary, at or near the top of the Fish Clay (Zone P1a, *Parvularugoglobigerina eugubina* missing) and at the contact of the Cerithium Limestone and overlying Bryozoan Limestone about 60 cm above the K/T boundary (part of Zone P1c missing). These unconformities are coeval with hiatuses observed in many continental shelf sections and indicate a global eustatic rather than regional isostatic response. Notable is that at Stevns Klint the episode of oceanic instability is registered over approximately the same stratigraphic interval in which supposed extraterrestrial amino acids occur, a circumstance that may indicate a connection.

A gradual positive shift in $\delta^{13}C$ is registered in both benthic and planktic foraminiferal assemblages in the upper Maastrichtian at Stevns Klint. The positive shift is followed by a prominent negative $\delta^{13}C$ shift (1.3‰) at the K/T boundary. An upper Maastrichtian positive $\delta^{13}C$ excursion followed by a negative $\delta^{13}C$ anomaly at or near the K/T boundary has previously been observed in deep-sea cores from the Pacific Ocean and the Weddell Sea, Antarctica, implying a global event. Previous suggestions of a relation between the uppermost Maastrichtian positive $\delta^{13}C$ excursion and sea-level variation are not supported by the data for Stevns Klint.

Introduction

During the past decade it has been intensively debated to what extent the profound change in fauna and flora that took place across the Cretaceous–Tertiary (K/T) boundary was a "gradual" or an "instantaneous" event. Proponents of a sudden event have suggested that the Maastrichtian was terminated by an earth-impacting asteroid that led to the sudden extinction of Cretaceous biota (Alvarez et al., 1980, 1984a; Smit and Ten

Correspondence to: B. Schmitz, Department of Marine Geology, Box 7064, University of Gothenburg, S-402 32 Gothenburg, Sweden.

0031-0182/92/$05.00

Kate, 1982; Smit, 1990). In contrast, proponents of a more gradual transition claim that, although an impact may have occurred, there were important long-term environmental changes at the K/T boundary that cannot be explained by an asteroidal impact alone (Ekdale and Bromley, 1984; Brinkhuis and Zachariasse, 1988; Keller, 1988a, b, 1989a, b; Sweet et al., 1990; Schmitz et al., 1991; Thierstein et al., 1991). The gradual environmental changes, rather than the impact alone, may be indicative of the primary mechanisms that led to mass extinctions of Cretaceous animal and plant species. Processes that took place at the K/T boundary, but which are not accounted for by the Alvarez et al. (1980) impact scenario are, for example, the prominent sea-level fluctuations registered in many shallow-water sequences (Hallam, 1987; Jones et al., 1987; Brinkhuis and Zachariasse, 1988; MacLeod and Keller, 1991a, b; Keller, in press), and extinctions of planktic foraminifera and nannoplankton both before and after the K/T boundary bolide event (Perch-Nielsen et al., 1982; Jiang and Gartner, 1986; Keller, 1988a, 1989a, b; Pospichal and Wise, 1990). Other protracted events include suppression of oceanic surface-water phytoplankton productivity variously estimated during 100–500 kyr (Boersma et al., 1979; Zachos and Arthur, 1986; Keller and Lindinger, 1989; Zachos et al., 1989; Stott and Kennett, 1989; Barrera and Keller, 1990), and long-term clay or marl formation in marine environments where chalks otherwise dominated (Schmitz, 1988, 1990a, b; Schmitz et al., 1991).

The determination of the precise spatial and temporal relationships between the K/T boundary bolide impact and the ongoing oceanic processes will be crucial for our understanding of the K/T boundary event. These relationships can best be studied in shallow-water successions with high sedimentation rates where stratigraphic resolution is significantly higher than in the deep sea (see MacLeod and Keller, 1991a, b). Detailed studies of paleoenvironmental changes across marine K/T boundary shallow-water sections with well-constrained iridium anomalies have been published, for instance, for El Kef, Tunisia (Brinkhuis and Zachariasse, 1988; Keller, 1988a, b; Keller and Lindinger, 1989), and Brazos River in Texas (Keller, 1989a, b; Barrera and Keller, 1990), but more information on additional sites is needed. Accordingly, we here present the results of a study of the shallow-water K/T transitional section at Stevns Klint in Denmark, where we have studied the distribution of benthic and planktic foraminifera and stable isotopes ($^{18}O/^{16}O$, $^{13}C/^{12}C$) in monospecific benthic and planktic foraminifera assemblages as well as bulk rock samples.

The sediments at Stevns Klint consist mainly of nannofossil chalks and bryozoan limestone that were deposited in an epicontinental sea at depths of 100–250 m, well below wave base (Håkansson et al., 1974; Bromley, 1979). A prominent sea-level fall is registered in the uppermost part of the Maastrichtian section (Rosenkrantz, 1937; Bromley, 1979; Ekdale and Bromley, 1984). The end-Cretaceous faunal and floral extinctions are well recorded at Stevns Klint and have been discussed, for example, in the symposia volume edited by Birkelund and Bromley, (1979). In the decade following the formulation of the asteroid impact hypothesis (Alvarez et al., 1980), studies dealing with the Stevns Klint section have been primarily concerned with the origin of its K/T boundary clay (the Fish Clay). Some authors have suggested that the clay represents ejecta fallout from an asteroidal impact (Alvarez et al., 1980; Kyte et al., 1980; Smit and Ten Kate, 1982; Kastner et al., 1984), whereas others support a predominantly local origin of the clay (Rampino and Reynolds, 1983; Schmitz, 1988, 1990a, b; Elliot et al., 1989). Ekdale and Bromley (1984) observed a transitional contact between the Fish Clay and the underlying chalk. This circumstance together with ichnofossil evidence for a late Maastrichtian sea shoaling, led them to reject the asteroid impact hypothesis and argue that sea-level changes associated with extensive volcanism better explains the gradual K/T boundary changes at Stevns Klint. Rochia et al. (1984, 1987), showing that the Ir anomaly at Stevns Klint begins about 70 cm below the K/T boundary, also favor a gradual K/T event and suggest that the protracted Ir anomaly may reflect the passage of the Earth through an interstellar dust could. Diffusion of Ir from the boundary clay, however, could not be excluded. Recently, Zhao and Bada (1989) discovered amino acids of supposed extra-

terrestrial origin in the section. The amino acids occur from about 1 m below to 0.3 m above the K/T boundary. In the boundary clay itself, however, no amino acids were found. Zahnle and Grinspoon (1990) suggest that this "long-term" imprint on the Stevns Klint K/T boundary sequence, was induced by some extraterrestrial process such as the capture in the inner solar system of a giant dust-carrying comet, of which a fragment struck the Earth at K/T boundary time.

The results of the present study indicate that the K/T boundary bolide impact event took place during a 100–500 kyr long period of anomalous instability in the sea at Stevns Klint. Over this period there occurred a succession of sea-level fluctuations and changes in bottom-water temperature and carbon-13 composition of sea water. Here we document these changes and discuss how they may relate to the K/T boundary bolide impact event.

Samples and methods

All samples were collected from different outcrops (depending on accessibility) in the sea-cliffs in the area 100–450 m south of the Højerup Church. Samples were collected with reference to distance above or below the deepest part of a Fish-Clay filled interbiohermal trough. For detailed information on the position of the samples in relation to different bioherm structures, see Fig. 1. Samples were collected over the interval from 7.2 m below to 2 m above the K/T boundary clay. Across the bulk part of the section sample intervals average approximately 1 m, however, in a 1 m interval centered across the K/T boundary, samples were collected at 10, 2, 1 or 0.5 cm intervals, with the closest spacings in the boundary clay. Across the boundary clay samples were collected so that the isotopic and foraminiferal results can be readily compared with microstratigraphic

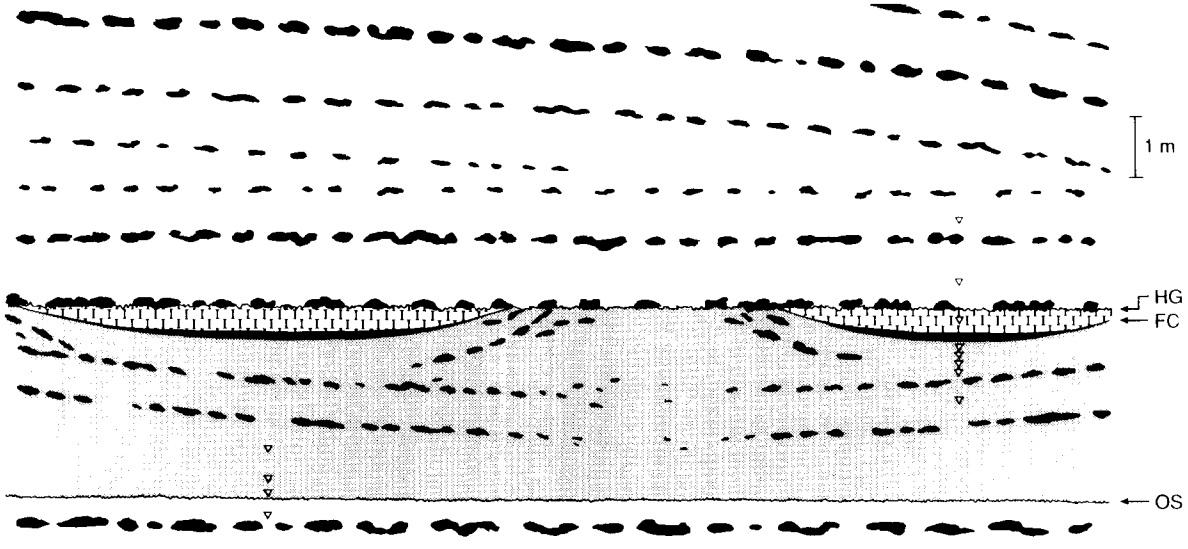

Fig. 1. Generalized sketch of the upper part of the studied K/T boundary section. The most important flint layers and two interbiohermal basins with Fish Clay are shown. In the about 3 m thick upper Maastrichtian greyish-white chalk the stratigraphy may be complex with overlapping mound structures (see also sketch by F. Surlyk in Alvarez et al. 1984b). In studies of this interval it is important to consider in detail the location of sampling places in relation to different bioherms. In this study we collected samples from the greyish-white chalk at two localities, 100 respectively 300 m south of the Højerup Church. As reference levels we used two prominent flint horizons together with the base of the Fish Clay (in the deepest part of the clay-filled interbiohermal troughs) and the transition from white to greyish-white chalk about 2.7 m below the K/T boundary. The two reference flint horizons can be found at many sites along the Klint near the Højerup Church. The flint layers occur in general about 70 cm respectively 140 cm below the base of the Fish Clay basins. Samples in the interval from 1 m below up to 2 m above the K/T boundary were collected at the site nearest to the Højerup Church, whereas samples in the interval from 1.7 to 2.9 m below the boundary were collected further south. (*FC* = Fish Clay; *HG* = hard ground; *OS* = omission surfaces; triangles = sampling places).

major and trace element profiles previously established by Schmitz (1988). Owing to constant erosion of the sea cliffs by the sea, the bedrock at Stevns Klint is normally fresh and unaltered. Despite this we removed at least 20–30 cm of outer sediment before sampling.

Samples were disaggregated in distilled water then washed through a sieve with a 63 μm mesh size. Relative abundances of both planktic and benthic foraminifera are based on sample counts of about 300 individuals per sample for each group in the size fraction greater than 63 μm. The remaining residue was searched for rare species. The >63 μm size fraction was chosen because of the multitude of small species which would be lost if the larger more standard (>125 μm or >150 μm) size fraction were used. All specimens were mounted on microslides for a permanent record and identified. Faunal census data are shown in Tables 1 and 2.

TABLE 1

Relative percent abundances of planktic foraminifera at Stevns Klint in size fraction >63 μm

	Upper Maastrichtian												
Sample number	1	2	3	4	5	6	7	8	9	10	11	12	13
Depth (in m, cm)	7.2 m	6.2 m	5.2 m	4.2 m	2.9 m	2.55 m	2.2 m	1.7 m	1.0 m	50 cm	40 cm	30 cm	20 cm
Globigerinelloides aspera	6	8	6	11	6	8	2	3	6	3	5	4	2
Globigerinelloides multispina	x	x	x	x	x	x	x	x		x	x	x	
Globigerinelloides volutus	x												
Globotruncanella havanensis			x	x		x	x	x		x			x
Globotruncanella subcarinatus	x	x			x								
Globigerina monmouthensis										x			
Hedbergella holmdelensis	8	4	6	x	2			x	x	x	x	x	x
Hedbergella monmouthensis	7	5	5	4	7	x	x	x	4	5	2	3	4
Globotruncana arca	x												
Globotruncana sp. (juveniles)													
Rugoglobigerina macrocephala													
Rugoglobigerina pennyl													x
Rugoglobigerina rugosa		x			x					x	x		x
Heterohelix complanata	19	18	17	16	21	16	24	18	24	13	16	29	15
Heterohelix globulosa	52	57	53	58	53	56	50	60	51	57	64	48	67
Heterohelix glabrans	x												
Heterohelix pulchra	x	x	x			x				x	x	x	x
Planoglobulina brazoensis			x		x	x	x	x					
Planoglobulina carseyae				5	2	x			2				x
Pseudotextularia cf. *elegans*			x										
Guembelitria cretacea	x	x	x	x	2	9	11	8	5	10	3	6	4
Guembelitria danica		2	7	x	3	7	9	4	7	9	6	7	5
Guembelitria trifolia													
Woodringina hornerstownensis													
Woodringina sp.													
Globoconusa daubjergensis													
Globoconusa conusa													
Eoglobigerina danica													
Eoglobigerina eobulloides													
Eoglobigerina taurica													
Subbotina pseudobulloides													
Unidentified	x												
Number of specimens counted	325	382	297	227	337	380	343	336	282	356	334	286	326

Sample 24 with parenthesis indicates actual number of specimens (rather than percent) present.

For stable isotope analysis monospecific foraminiferal samples in the size fraction between 125–250 μm were collected of the planktic species *Heterohelix globulosa* and the benthic species *Cibicidoides succedens*. In addition to monospecific foraminifers, assemblages of mixed benthic species were analyzed from 7.2 m below to 6 cm above the boundary; *C. succedens* was the most common species in these polyspecific samples. Also analyzed were single very large (> 500 μm) individuals of *C. succedens* from a few stratigraphic levels. In the 15-cm-thick interval immediately below the boundary we analyzed monospecific assemblages of *Rugoglobigerina rugosa*, and two size fractions of *C. succedens* (125–185 μm and 185–250 μm). The latter analyses were performed in order to rule out any size effects on the isotopic results. For each isotopic analysis about 0.3–0.5 mg of foraminifera were used. This means that about 200 individuals of *H. globulosa* had to be picked for each analysis.

							Danian P1c						
14 15 cm	15 9–11 cm	16 8–10 cm	17 6–8 cm	18 4–6 cm	19 2–4 cm	20 0–2 cm	21 0–1 cm	22 2–4 cm	23a 4–6 cm	23b 5–7 cm	24 25 cm	25 1 m	26 2 m
3	7	2	3	3	4	6				5	(1)		
	x					x							
		x										x	
x		x		x	x	x							
x		x		x	x						(1)		
x		x	x	x	x	x					(1)		
2	4	3	2	x	2	2				8			
x	x												
x	x		x	x	x	x							
2	3	3	7	7	4	12				2			
20	20	14	20	15	11	7				7	(4)		
58	57	70	58	64	60	64				64	(2)	x	
x	x		x	x	x	x							
				x		x							
x			x			x				x			
2	3	2	2	2	5	x				x	(4)	8	9
3	x	x	2	2	4	2				x	(1)		
			3	x	2	x				3			22
										x			4
											(3)		
											(2)	42	34
										x			
										4	(4)	28	17
												x	x
											(5)	19	10
													2
		x			x	2							
353	209	298	319	365	309	501	(no planktic foram.)				28	145	246

TABLE 2

Relative percent abundances of benthic foraminifera at Stevns Klint in size fraction > 63 μm

Sample number Depth (in m, cm)	Upper Maastrichtian										
	1 7.2 m	2 6.2 m	3 5.2 m	4 4.2 m	5 2.9 m	6 2.55 m	7 2.20 m	8 1.70 m	9 1.00 m	10 50 cm	11 40 cm
Alabamina midwayensis Brotzen	x	x				x	x	x	x		
Allomorphina trochoides (Reuss)	x	x	x		x	x		x		x	
Anomalinoides praeacuta (Vasilenko)									x		
Anomalinoides welleri (Plummer)	5	x	8	3	2	2	2	3	2		x
Angulogerina cuneata Brotzen	x	3	x	5	6	7	6	2		x	x
Astacolus sp.										x	x
Bolivinoides decorata (Jones)											
Bolivinoides decurrens (Ehrenberg)	x	x	x		x	x					x
Bolivinoides draco (Marsson)	3	x	2	6	6	9	7	13	x	5	3
Bolivinoides paleocenica Brotzen											
Cassidulina globosa Hantken	x						3	2	x		x
Cibicidoides alleni (Plummer)	4	4	7	6	x	3	x	4	3	4	4
Cibicidoides succedens (Brotzen)	5	11	13	12	7	8	6	12	7	14	12
Cibicidoides cf. *newmanne*			x	x		x			3	x	
Conorbina minuta (Sliter)	x			x		x					
Coryphostoma incrassata (Reuss)	x	x	x	x	x				x	2	3
Coryphostoma plaitum (Carsey)	x	x	x	x	x						
Dentalina sp.	x		x	x		x			x	x	
Dorothia oxygona (Reuss)	x					x	x	x	x		
Epistominella minuta (Olsson)	3	3	8	6	5	7	5	x	6	3	x
Eponides lunatus (Brotzen)			x	x	x	x	x		x		
Frondicularia sp.				x			x				
Fursenkolna sp.		x			x	x		x			
Gavelinella danica (Brotzen)											
Gavelinella lillingensis (Brotzen)	x			x	x	x				x	x
Gavelinella involuta (Reuss) (Brotzen)	6	4	3	x	9	3	13	7	4	3	8
Gavelinella cf. *sandigel* (Brotzen)		x	x	x	2	x	2	x	x	x	x
Gaudryna pyramidata Cushman						x					
Globulina lacrima (Reuss)			x	x	x	x		x		x	
Globulina subsphaerica (Berthelin)		3	x			x			x		x
Gyroidinoides depressus (Alth)				x	2	x	x	x	x		
Gyroidinoides orbicularis (d'Orbigny)		9	3								
Gyroidinoides girardanus (Reuss)	2	x		x	2		x	x	x	x	x
Gyroidinoides subangulata (Plummer)	x				x	x			x	x	
Heterolepa cf. *minuta* Sliter	3	3	x	x	x	x	x	x	x	x	
Lagena hispida Reuss				x							
Lagena paucicostata Franke					x	x	x	x		x	x
Lagena sulcata (Walker & Jakob)				x	x		x				
Lagena sp.		x			x				x		
Lenticulina discrepans (Reuss)						x	x				
Lenticulina modesta (Bondy)			x		x				x	x	
Lenticulina muensteri (Roemer)					x	x				x	x
Lenticulina sp.	x			x	x			x	x	x	
Neoflabellina postreticulata Hofker				x						x	
Nonionella sp.	x		x		x	x				x	
Oridorsalis umbonatus (Reuss)			x	x		x		x	x	x	x
Osangularia lens	12	5	4	4	7	6	3	13	24	18	24
Pleurostomella subnodosa Reuss						x					

									Danian P1c					
12 30 cm	13 20 cm	14 15 cm	15 9–11 cm	16 8–10 cm	17 6–8 cm	18 4–6 cm	19 2–4 cm	20 0–2 cm	21 0–1 cm	'22 2–4 cm	23 4–6 cm	24 25 cm	25 1.00 m	26 2.00 m
	x		x			x						x		
x	x	x	x		x	x	x	x			x			
			x			x	x	x			x	4		
x	x	2	x	x	2	2	x	x					2	2
x		x		x	2		x	x						
		x				x						x		
			x	x		x		x						
x			3		x	x	x	x						
3	3	x	5	3	2	3	2	3						
											x	6	2	
x	x								16	15	x	x	3	
5	2	5	4	5	x	2	2	4	21	38	37	19	32	14
12	7	15	10	14	11	18	9	20						
2	5	3	2											
		x		x		x		x					x	
2	x	x	x	x		x		x					x	
x				x							x			
	x				x	x								
x	x	x	x		x	x								
4	4	x	x	3	4	4	9	2						
		x	x	x	x			x						
				x	x			x						
	x	2				x							x	
x					x								x	
5	6	x	5	3	3	4	5	2					6	x
x	x		x	x	2	x	2	x		2	5	2	4	6
x				x										
			x		x	x		x				x	x	x
x	x		x	x	x	x	x	x				x		
														3
x	x				x		x	x						
x		x		x										
x	x		x	x	x	x		x						
			x				x					x		
			x											
	x							x						x
	x			x				x	x				x	
	x	x	x	x			x	x	x			x	x	
x	x			x	x				x	x				
x		x			x	x				x	x			
							x					x		
x	2	x	x		x	3	x	2		x	3	x	2	
18	31	21	28	25	22	17	26	29	25	22	17	26	29	61

TABLE 2 (*continued*)

Sample number Depth (in m, cm)	Upper Maastrichtian										
	1 7.2 m	2 6.2 m	3 5.2 m	4 4.2 m	5 2.9 m	6 2.55 m	7 2.20 m	8 1.70 m	9 1.00 m	10 50 cm	11 40 cm
Praebulimina aspera Cushman & Parker	7	7	7	3	13	6	6	6	x	x	2
Praebulimina carseyae (Plummer)	15	17	17	9	12	13	13	7	13	8	11
Praebulimina cushmani (Sandidge)	x	x	x	x	x	2	3	4	5	11	4
Praebulimina quadrata (Plummer)						x					
Praebulimina cf. *reussi* (Morrow)							x		x	x	2
Praebulimina sp.	x										
Pullenia cretacea Cushman	x	x	x	x	x	x	x	x	x	x	x
Pullenia jarvisi Cushman	x	x		x	x	x	x	x	x		
Pulsisiphonina prima (Plummer)									x		
Pyramidina cimbrica (Troelsen)	x	x	x	x	x	2	4	2	6	3	9
Pyramidina rudita (Cushman & Parker)	3	6	3	4	4	2	x	x	x	x	
Pyrulina sp.											
Quadrimorphina camerata (Brotzen)							x	x			
Quadrimorphina profunda Schnitker & Tjaisma	2		x	x	x	x	x	x			x
Rosalina koeneni Brotzen			x		x	4	x	4	x	4	x
Rosalina ystadensis Brotzen					x			x			x
Rosalina sp.											
Spirillina subornata Brotzen		x	x	x		3	4	7	4	x	x
Stensioeina pommerana Brotzen	x	x	x	3	x	x	x	x	3	3	2
Stilostomella spinosa Hofker			x								x
Tappanina selmensis (Cushman)	9	13	x	10	7	5	3	x	x	x	x
Trifarina esnehensis Le Roy	x										
Tristix excavata (Reuss)											
Unidentified		x			x	x				x	x
Number of specimens counted	271	264	216	317	315	342	243	189	214	303	251

The corresponding numbers for *R. rugosa* is 150 individuals and for *C. succedens* 60 individuals in the size range 125–185 μm and 30 with sizes 185–250 μm. In some sublayers of the Fish Clay foraminifera are very rare and considerable effort was expanded to collect the requisite number of specimens.

Bulk-rock isotopic analyses were performed on all samples from which foraminiferal assemblages had been recovered. We ground a few grams of each sediment sample to a fine-grained well-mixed powder and then separated about 0.3–0.7 mg of material for analysis.

All picked foraminifera for isotopic analysis were ultrasonically cleaned in methanol and thereafter roasted in vacuo at 400°C for 30 minutes. Carbon dioxide was released by reaction with 100% orthophosphoric acid at 50°C. The gas was dried in two steps with solid CO_2 and ethanol and thereafter directly transferred by the action of liquid N_2 to a VG Micromass 903E mass spectrometer. Calibration of analytical data was made against the standard NBS-20, which is assumed to have values of $-4.14‰$ for $\delta^{18}O$ and -1.06‰ for $\delta^{13}C$. Data were normalized against PDB using the δ notation. Replicate analyses of the NBS-20 standard gave a standard deviation of $\pm 0.03‰$ for $\delta^{13}C$ and $\pm 0.04‰$ for $\delta^{18}O$.

Lithostratigraphy and biostratigraphy

Along the sea cliffs at Stevns Klint about 50–60 m of the K/T transitional stratigraphic record can be studied. In summary, the cliffs are built up of: (1) a basal, more than 10 m thick section of white chalk with bryozoa fragments deposited as low mounds; (2) about 20 m of white chalk in horizontal beds with only rare bryozoa fragments; (3)

									Danian Plc					
12 30 cm	13 20 cm	14 15 cm	15 9–11 cm	16 8–10 cm	17 6–8 cm	18 4–6 cm	19 2–4 cm	20 0–2 cm	21 0–1 cm	22 2–4 cm	23 4–6 cm	24 25 cm	25 1.00 m	26 2.00 m
2	x	3		x	x	x			x	x	x			
10	7	4	4	4	11	9	8	9	4	11	9	8	9	
4	x	7	2	2	3	6	x	5	2	3	6	x	5	
x	x													
					x					x				
x				x	x	x		x	x	x	x		x	
			x	x		x		x	x		x		x	
7	11	12	9	11	13	4	8	x	11	13	4	8	x	
x	2	2	2	3	x	2	4	2	3	x	2	4	2	
				x					x					
						x	x				x	x		
x				x	x		x		x	x		x		
3	2	x	5	x	7	5	4	x	x	7	5	4	x	
				x					x					
3	2	2	x			x	x				x			
3		2	2	2	3	x	x	4	2	3	x	x	4	
				x					x					
x	2	4	2	x	2	x	4	x	x	2	x	4	x	
			x											
		x	x	x		x			x		x			x
274	225	155	270	214	266	304	236	327	214	266	304	236	327	57

about 2–3 m of greyish white, bryozoan-rich chalk in undulating bioherms; (4) 0–0.2 m of grey-brown to black, pyrite-rich Fish Clay in the bottoms of interbiohermal troughs; (5) a 0–0.1 m thick marl layer containing chalk fragments; (6) 0–0.5 m of yellow-white Cerithium Limestone; (7) a prominent hardground associated with a 0–0.1 m thick conglomeratic layer; and (8) up to 20 m of cream-colored bryozoan-rich limestone in large, asymmetrical bioherms (Rosenkrantz, 1937; Surlyk, 1979; Alvarez et al., 1984b; Ekdale and Bromley, 1984; this study). Within the interval studied by us (from 7.2 m below to 2 m above the K/T boundary) there are at least three hiatuses, each associated with a change in lithology.

Latest Maastrichtian hiatus

In the studied section the first hiatus occurs about 2.7 m below the deepest part of the Fish Clay basins, at the contact between the horizontal white chalk beds (~ 20 m thick) with rare bryozoan fragments, and the overlying, undulating grey-white chalk beds rich in bryozoans (Fig. 1; see also Surlyk, 1979). Stratigraphically this hiatus is within the *Pseudotextularia elegans* planktic foraminifer Zone and the *Palynodinium grallator-Chiropteridium inornatum* dinoflagellate Zone (Hultberg and Malmgren, 1987). Thus, the temporal extent of this hiatus can not be determined based on the present microfossil stratigraphy. However, major planktic and benthic foraminiferal changes across this lithologic contact (discussed later) suggest that a significant interval of time may be missing.

K/T boundary Fish Clay

Hansen (1978) argued that a major hiatus also occurs at the base of the Fish Clay, based on the

absence of the *P. grallator–C. inornatum* dinoflagellate Zone. A reexamination of this section by Hultberg and Malmgren (1987) revealed, however, that this dinoflagellate zone is both present and has an unusually great vertical extent in the Stevns Klint section. Hultberg and Malmgren (1987) therefore argued that no hiatus is present at the base of the Fish Clay and, moreover, that this is one of the most complete *pre-K/T* boundary sections in the Danish basin. The present study supports their latter conclusion as foraminiferal changes are gradual through the 2.7 m of the grey-white chalk beds underlying the Fish Clay. Because of poor fossil preservation and dissolution, microfossil stratigraphy cannot determine whether sedimentation across the contact with the Fish Clay is temporally continuous, or represents some interval of non-deposition. Based on lithologic evidence, Rosenkrantz (1966), Ekdale and Bromley (1984) and Schmitz (1988) considered the lower contact of the Fish Clay with chalk as transitional indicating continuous sedimentation. During formation of the Fish Clay, however, sedimentation may have been extremely condensed (Schmitz, 1990b).

Early Danian hiatus

Planktic foraminiferal stratigraphy indicates that a hiatus is present at the top of the Fish Clay. Lithologically this hiatus may be indicated by the marl with chalk fragments that separates the Fish Clay from the overlying Cerithium Limestone (see Christensen et al., 1973). Unfortunately, the temporal extent of this hiatus cannot be estimated precisely because planktic foraminifera are absent in the boundary clay, due to dissolution, and poorly preserved above this interval. Nevertheless, some indications as to the duration of this hiatus can be obtained from foraminiferal stratigraphy as discussed below.

The first Tertiary planktic foraminifera were found in a sample collected in the transition interval between the Fish Clay and the Cerithium Limestone. This sample contained an essentially Cretaceous faunal assemblage similar in species composition and abundances to samples immediately below the boundary clay. However, in the fine fraction (38–63 μm) it also contained the Tertiary species *Woodringina hornerstownensis, Globoconusa conusa* and *Eoglobigerina danica* which indicates that deposition occurred in the early Danian and that the predominantly Cretaceous fauna was probably reworked. In the absence of the planktic foraminiferal index species *Parvularugoglobigerina eugubina*, deposition of this sample may have occurred as early as Zone P0, or as late as Zone P1b or base P1c. The sample that we collected in the upper part of the Fish Clay (4–6 cm above its base) is barren of planktic foraminifera and could have formed at any time between Zone P0 or base P1c. The sample from the Cerithium Limestone, at 25 cm above the K/T boundary, contains very rare and poorly preserved Cretaceous and Tertiary planktic foraminifera including the Tertiary species *Woodringina sp., Globoconusa daubjergensis, Eoglobigerina danica* and *Subbotina pseudobulloides* (Table 1). These taxa, in the absence of *P. eugubina, Eoglobigerina taurica* and well developed *G. daubjergensis*, indicate a P1b or lower Zone P1c age.

This stratigraphic information suggests the presence of an early Danian hiatus near the top of the Fish Clay that at a minimum spans the whole or a substantial part of the P1a (*P. eugubina*) Zone and at a maximum spans from within Zone P0 to within the lower part of Zone P1c.

Hiatus at contact between Cerithium and Bryozoan Limestones

A prominent lithologic unconformity associated with a conglomerate is recognized between the Cerithium Limestone and the Danian bryozoa-rich limestone about 0.6 m above the K/T boundary in our section (Surlyk, 1979; Alvarez et al. 1984b; this study). Current planktic foraminiferal data is inconclusive regarding the extent of this hiatus. However, a sample at 1 m above the boundary clay contains abundant *S. pseudobulloides* and *G. daubjergensis*, which indicate a Zone P1c age (Fig. 2, Table 1). The data thus suggest that the hiatus formed within planktic foraminiferal Zones P1b or P1c or at the transition between these two zones.

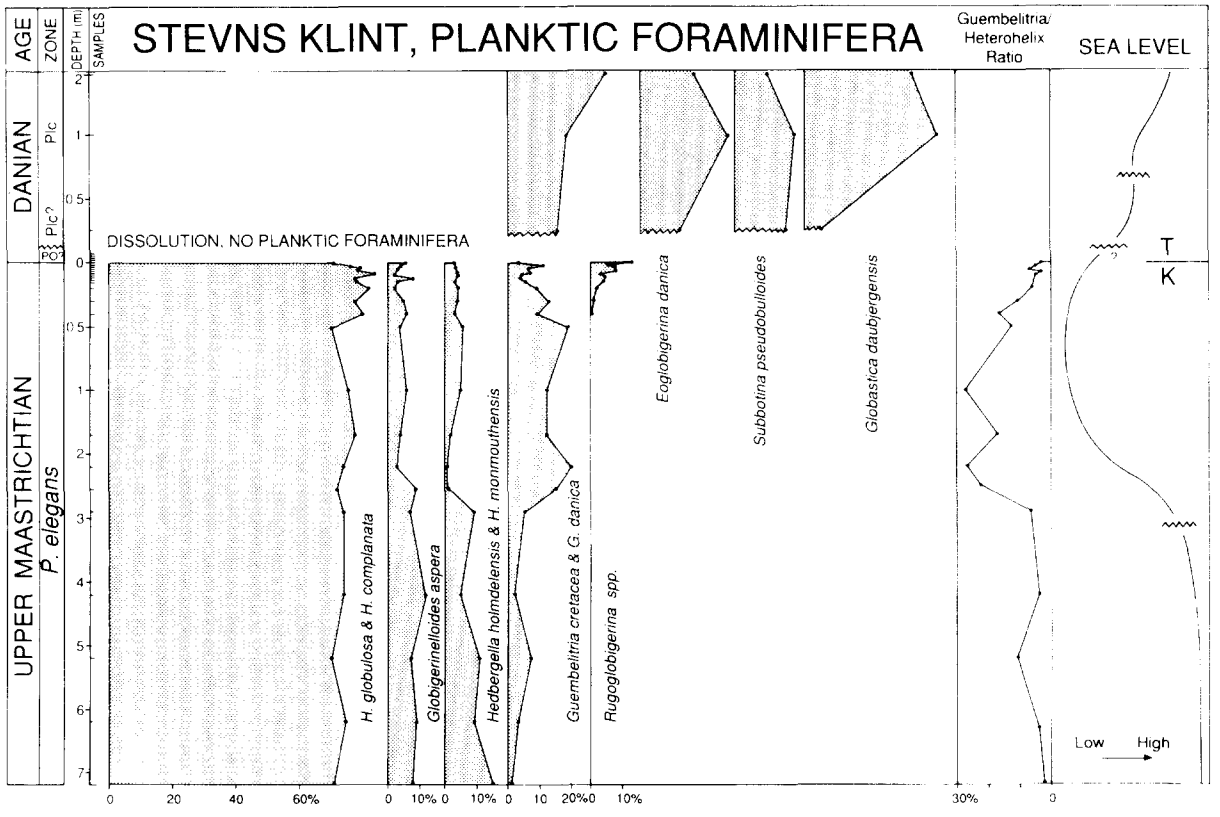

Fig. 2. Distribution of planktic foraminifera across K/T boundary section at Stevns Klint.

Sedimentation rates

Sedimentation rates at Stevns Klint have previously been suggested to be about 10 cm per 1000 years (Håkansson et al., 1974; Kaminski and Malmgren, 1989). This number has been calculated by dividing the maximum thickness of the Maastrichtian deposits (700 m; Stenestad, 1971) in the Danish–Polish trough with the duration of the Maastrichtian eon (7.5–8 Ma; Kent and Gradstein, 1985). Considering, however, the discontinuous nature of sediment deposition in most marine environments (MacLeod and Keller, 1991a, b), sedimentation rates may have been higher across the continuous intervals of the Stevns Klint section. It must also be considered that different parts of the section, most likely, formed at different rates. For example, the uppermost Maastrichtian and Danian bryozoa bioherms may have formed at a substantially higher rate than the bryozoa-poor chalk deposits further down in the section.

Assuming average sedimentation rates of 10–20 cm per 1000 years for Stevns Klint, the 10-m thick section studied by us represents sediment accumulation during 50–100 kyr. Considering, however, that the section contains index foraminifera from the uppermost Maastrichtian and up to Zone Plc, and using geochronological estimates of the duration of this biostratigraphic interval (Berggren et al., 1985; MacLeod and Keller, 1991b) suggest that, from bottom to top, the section spans a time interval of several 100 kyr. Apparently the hiatuses in the section represent a substantial amount of time (see also MacLeod and Keller, 1991a, b).

Foraminiferal analyses

Distribution of planktic foraminifera

The upper Maastrichtian planktic foraminiferal fauna at Stevns Klint is of low diversity and

dominated by a few cosmopolitan taxa of the genera *Heterohelix, Hedbergella, Guembelitria* and *Globigerinelloides*. This low diversity dominant fauna is characteristic of continental shelf environments and is similar to the dominant fauna in the Brazos River sections of Texas (Keller, 1989a, b). Two significant faunal changes occur in the upper Maastrichtian at Stevns Klint (Fig. 2). The first major faunal change occurs at about 2.7 m below the K/T boundary, at the base of the grey-white bryozoan-rich chalk, which marks an unconformity as discussed earlier. The second faunal change begins at about 40 cm below the K/T boundary. Isotopic ranking of planktic foraminifera in the water column suggests that these faunal changes indicate a maximum sea level fall between 2.7 m and 0.5 m below the K/T boundary and the onset of a sea level rise beginning about 0.4 m below the K/T boundary as discussed below.

Planktic foraminifera primarily live in the upper 200–400 m of the water column and within this interval are depth stratified as shown by stable isotope ranking of individual species (Douglas and Savin, 1978; Boersma and Shackleton, 1981; Stott and Kennett, 1989; Keller, 1985; Keller et al., 1992). In the Cretaceous ocean large taxa (globotruncanids, planoglobulinids, pseudotextularids) generally lived in deeper waters, whereas small taxa (heterohelicids, guembilitrids, hedbergellids, globigerinelloids) generally lived in the upper 100–200 m of the water column. This depth stratification tends to result in the exclusion of deeper water taxa, including the late Maastrichtian index species *Abathompalus mayaroensis*, from shallow continental shelf and intracratonic regions in both high and low latitudes, as is the case at Stevns Klint, El Kef and Brazos River sections (Keller, 1988a, 1989a, b). As a result, late Maastrichtian sediments in shallow water regions are assigned to the *Pseudotextularia elegans* Zone (Malmgren, 1981) or the *P. deformis* Zone (Keller, 1988a).

Among the shallow water taxa, *Guembelitria* is consistently the isotopically lightest group and is inferred to live closest to the ocean surface (Kroon and Nederbragt, 1990; Barrera and Keller, unpublished data), whereas the isotopically heavier *Heterohelix* group lives slightly deeper (Stott and Kennett, 1989; Barrera and Keller, 1990) and hedbergellids and globigerinelloids live in still deeper waters. In contrast, rugoglobigerinids are open ocean surface dwellers (Boersma and Shackleton, 1981; Barrera and Huber, 1990). With this information it is possible to interpret sea-level fluctuations from relative species abundance changes at Stevns Klint.

Two heterohelicid species, *H. globulosa* (50–70%) and *H.* cf. *complanata* (10–20%), dominate the Upper Maastrichtian assemblages, but show no major variations up to 40 cm below the K/T boundary where they increase in abundance (Fig. 2). (*H. globulosa*= *H. striata* of Hultberg and Malmgren (1986, 1987); this species is identified as *H. globulosa* because it lacks the characteristic strong striations of *H. striata*). Both *Guembelitria* and *Heterohelix* are generally dominant in continental shelf regions and decrease in abundance in open marine environments (Sliter, 1972; Hultberg and Malmgren, 1986, 1987; Keller, 1988a, 1989a,b; Kroon and Nederbrogt, 1990; D'Hondt and Keller, 1991). Thus, the high abundance of *Heterohelix* characterizes deposition in a shallow marine environment at Stevns Klint. In contrast to *Heterohelix*, the surface dweller *Guembelitria* (*G. cretacea, G. danica*) shows a major abundance increase from 4% to 20% between 2.7 m and 0.5 m below the K/T boundary and decreases again in the 40 cm below the K/T boundary (Fig. 2). At the same time, deeper water dwellers, *Globigerinelloides* (*G. aspera, G. multispina*) and *Hedbergella* (*H. holmdelensis, H. monmouthensis*), simultaneously decline in abundance at 2.7 m below the K/T boundary. In the 40 cm below the K/T boundary, the open marine surface dweller *Rugoglobigerina rugosa* rapidly increases.

The increase in the surface dweller *Guembelitria* and concurrent decline in deeper dwellers *Globigerinelloides* and *Hedbergella* beginning at 2.7 m below the K/T boundary are interpreted to indicate shallowing of the marine environment. In contrast, the decline in *Guembelitria* abundance and concurrent increase in the open marine surface dweller *Rugoglobigerina* beginning about 40 cm below the K/T boundary is interpreted as a sea level rise. These faunal interpretations are supported by the benthic foraminiferal changes as discussed below.

The paleobathymetric changes indicated by these

planktic foraminiferal species abundance changes can be summarized by values of the *Guembelitria/Heterohelix* (surface/subsurface) ratio (Fig. 2). High values of this ratio indicate shallower conditions, as exemplified by increased abundance of *Guembelitria* between 2.7 m and 0.5 m below the K/T boundary, whereas low values indicate deeper water as seen in the upper 40 cm of the Maastrichtian at Stevns Klint. This planktic paleobathymetric index correlates well with the sea level curve inferred from benthic foraminiferal assemblages as discussed below. Our interpretation contrasts, however, with that of Hultberg and Malmgren (1986) who used a *Globigerinelloides/Heterohelix* ratio as paleodepth indicator and concluded that there was shallowing during the uppermost meter of the Maastrichtian. Although their paleodepth index should, in theory, provide the same results as ours, the difference is probably due to a bias in their faunal census data. Hultberg and Malmgren (1986) used the larger size fraction (> 125 μm) in their faunal analysis which excludes small species such as *Guembelitria* and thus biases the results in favor of larger taxa. Moreover, the second paleobathymetric index used by Hultberg and Malmgren (1986), the abundance of *Spiniferites* dinoflagellate cysts, does not concur with their *Globigerinelloides/Heterohelix* index, and instead shows the same paleobathymetric trend as our *Guembelitria/Heterohelix* ratio.

In the basal Danian section planktic foraminiferal assemblages are poorly preserved and paleobathymetric interpretations (Fig. 2) are based on benthic foraminiferal assemblages and correlation with sea level changes observed at El Kef and Brazos River (Brinkhuis and Zachariasse, 1988; Keller, 1988a, b, in press).

Distribution of benthic foraminifera

Relative abundances of common benthic foraminiferal species across the K/T boundary at Stevns Klint are illustrated in Fig. 3. In the lower part of the section, between 7 m and 2.7 m below the K/T boundary, no significant faunal changes are observed. A major benthic faunal turnover, however, occurs correlative with the faunal turnover observed in planktic foraminifera, at the unconformity between the white chalk and overlying grey-white chalk about 2.7 m below the K/T boundary clay. In this interval the outer shelf taxa *Gyroidinoides* spp., *Angulogerina cuneata* and *Tappanina selmensis* decline in abundance and nearly disappear. Correlative with this abundance decline is an increase in the shallower mid-shelf taxa *Pyramidina cimbrica, Rosalina koeneni, Spirillina subornata* and *Praebulimina cushmani*. No clear trend is observed in other taxa at this interval. However, there is a further faunal change at about 1 m below the K/T boundary where the outer shelf taxa *Praebulimina aspera* and *Bolivinoides draco* permanently decline in abundance and *Stensioiena pommerana* and *Osangularia lens* increase (Fig. 3).

These benthic faunal abundance changes suggest that sea level was lowered substantially between deposition of the white chalk and bryozoan-rich grey-white chalk, as also observed in planktic foraminiferal assemblages, and probably continued to drop up to at least 1 m below the K/T boundary. In the intracratonic sea at Stevns Klint this sea-level fall probably resulted in shallowing from about 200 m to 100 m water depth. This is comparable to a change from an outer shelf to a middle shelf environment.

The onset of the subsequent sea level rise is not easily recognized in the benthic foraminiferal assemblages. However, there are some indications of a deepening sea in the abundance decline of *P. cushmani* beginning about 50 cm below the K/T boundary and especially in the reappearance of the deeper dwelling taxa *T. selmensis* and *A. welleri* about 20 cm below the K/T boundary (Fig. 3). The abundance increase in *P. cimbrica* during this interval may not be related to paleodepth changes.

The benthic foraminiferal changes across the K/T boundary and into the early Danian at Stevns Klint are difficult to evaluate because of severe carbonate dissolution beginning in the boundary clay which resulted in the presence of only a few very poorly preserved solution resistant taxa (e.g. *Cibicidoides succedens, C. alleni, Osangularia lens*). For this reason the relative abundances of these taxa are artificially inflated and do not represent their original relative abundances in the benthic

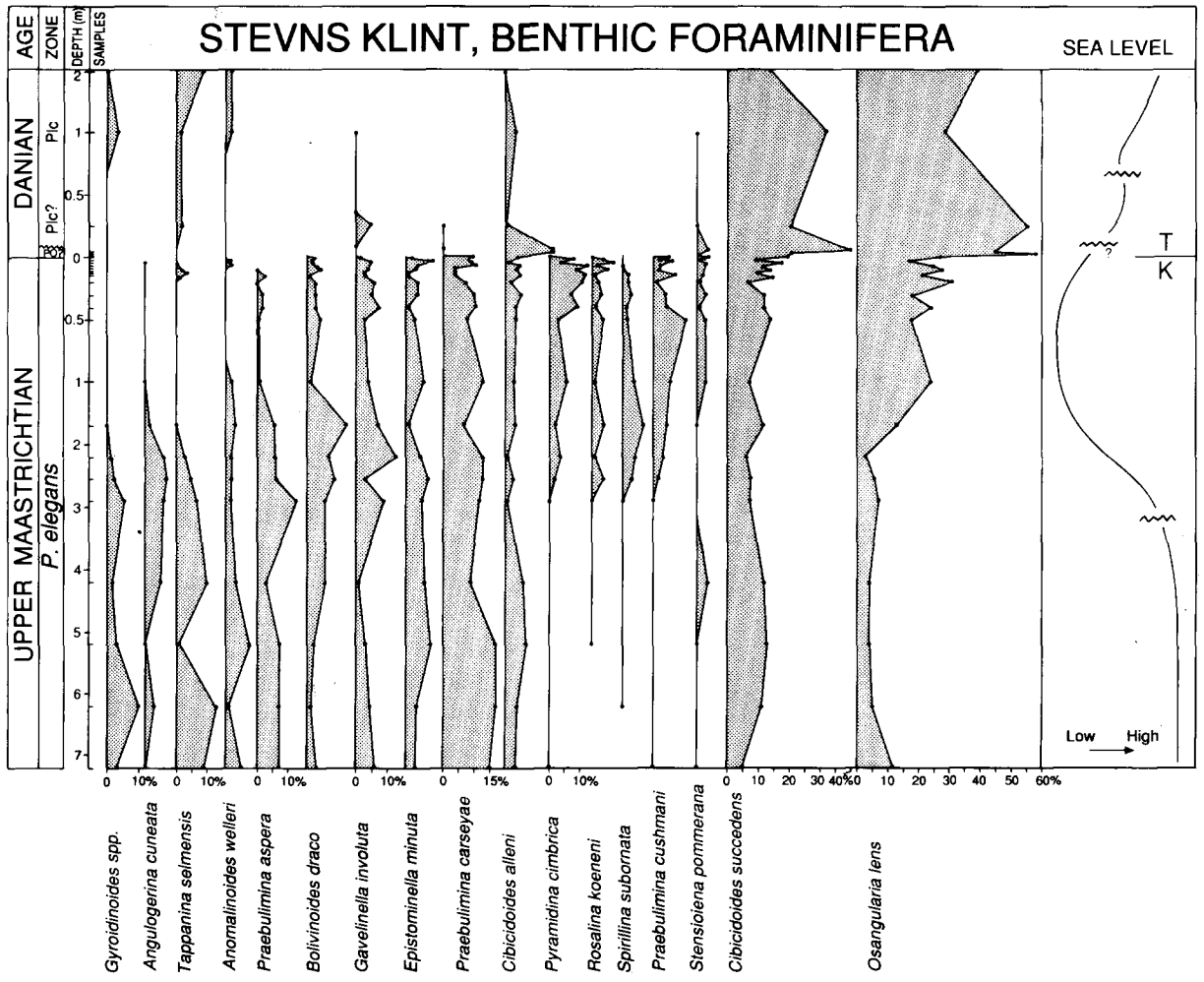

Fig. 3. Distribution of benthic foraminifera across K/T boundary section at Stevns Klint.

foraminiferal population. For the same reason, we can not assume that the disappearances of all the taxa at the base of the boundary clay represent extinctions at the K/T boundary (Fig. 3, Table 2). Despite the poor preservation, samples between 0.5 and 2 m above the K/T boundary contain increasing abundances of taxa indicative of an outer shelf environment (e.g. *Gyroidinoides* spp., *T. selmensis* and *A. welleri*) suggesting a continuing sea level rise into the Danian. A general sea level rise during the earliest Danian was also observed at El Kef, Tunisia (Brinkhuis and Zachariasse, 1988) and at Brazos River, Texas (Keller, 1989a; MacLeod and Keller, 1991a, b).

Stable isotope analyses

Preservation of foraminifera

Planktic and benthic foraminifera are generally well preserved and not recrystallized in the Maastrichtian sediments although dissolution effects are evident in the 2–3 cm interval immediately below the K/T boundary clay. Carbonate dissolution is strong in the boundary clay resulting in the presence of only large and generally fractured solution-resistant benthic taxa. Studies with the light microscope indicate, however, that the solution-resistant individuals consist predomi-

nantly of original calcite. Thus, stable isotopic data for Maastrichtian and K/T boundary foraminiferal samples are likely to represent original signals. This is corroborated by the isotopic results, which are consistent with a priori expectations as regards depth ranking of foraminifera etc. (discussed later). In the Danian, dissolution is less severe than in the boundary interval, however, foraminiferal shells are difficult to clean from adhering calcite crystals and some recrystallization of foraminiferal calcite is evident.

$\delta^{18}O$ record measured in foraminifera

The $\delta^{18}O$ records of the subsurface dwelling planktic foraminifer *Heterohelix globulosa*, the benthic foraminifer *Cibicidoides succedens* and mixed benthic species are illustrated in Fig. 4 and Tables 3–4. In the upper Maastrichtian from 7.2 m below up to the K/T boundary, *H. globulosa* shows relatively stable $\delta^{18}O$ values varying between $-1.7‰$ to $-2.0‰$. Mixed benthic and *C. succedens* samples show relatively stable $\delta^{18}O$ values near $-1.5‰$ from 7.2 m to 2.7 m below the K/T boundary, but increase gradually about 0.3‰ from between 2.7 m to 0.1 m below the K/T boundary. In the boundary clay $\delta^{18}O$ values of *C. succedens* increase additionally about 0.6‰ and then return to lighter values around $-1.3‰$ in the early Danian (Fig. 4). The $\delta^{18}O$ values of *C. succedens* and polyspecific benthic assemblages are very similar and in general show less than 0.1‰ difference. The similarity in isotopic values may be due to the fact that a large portion of the mixed benthic assemblage consists of individuals of *C. succedens* and the closely related *C. alleni*.

A closer examination of $\delta^{18}O$ values in the interval from 16 cm below to 6 cm above the K/T boundary is illustrated in Fig. 5 for the surface dweller *Rugoglobigerina rugosa*, subsurface dweller *H. globulosa* and mixed benthic foraminifers. In addition, *C. succedens* were analyzed over the same interval in two size fractions (125–185 μm, 185–250 μm) (Fig. 6). The K/T boundary was defined by the conspicuous 0.5 cm thick spherule-rich light brown to brownish red layer (hereafter referred to as "the red layer") immediately below the black clay layer (Schmitz, 1988).

Over the 3-cm interval that immediately underlies the red layer the mixed benthic assemblage and the surface dweller *R. rugosa* show a slight gradual shift towards more positive $\delta^{18}O$ values (Fig. 5). For *H. globulosa* and the two different size fractions of *C. succedens* no similar gradual pre-K/T change is observed (Figs. 5–6). The weak gradual trends for some of the foraminiferal assemblages below the boundary clay probably reflects contamination with bulk-rock calcite and/or dissolution effects. As discussed in the next section, bulk-rock calcite shows a strong gradual decline in $\delta^{18}O$ over the interval considered. Microscopical examination of the different foraminiferal assemblages revealed significant bulk-rock calcite infillings (despite extensive ultrasonic treatment) in individuals from the assemblages showing a gradual $\delta^{18}O$ decline. Moreover, Wu and Berger (1989) and Wu et al. (1990) have shown that because calcite dissolution removes thin-walled surface-dwelling foraminifera in preference of thick-walled deeper-living foraminifera, dissolution may result in a shift towards more positive $\delta^{18}O$ values even in monospecific foraminiferal assemblages. Because of dissolution effects the thin-walled *H. globulosa* becomes extremely rare already 2 cm below the boundary, whereas the more thick-walled *R. rugosa* can be found up to 0.5 cm below the boundary. It appears likely that dissolution effects and calcite infillings account for the gradual slight positive $\delta^{18}O$ shift for *R. rugosa* below the boundary clay.

Because of carbonate dissolution the K/T boundary clay is barren of planktic foraminifera, however, some partially dissolved benthic foraminifera can be found. Species identification of the fragmented foraminifera is difficult, and only after considerable efforts was it possible to analyze monospecific assemblages of *C. succedens* from two sublayers of the K/T boundary clay (Fig. 6). The isotopic results show a profound positive $\delta^{18}O$ shift (0.6‰) indicating a 3°C cooling of bottom waters during formation of the boundary clay. The mixed benthic assemblages also indicate cooling (Fig. 5), however, these results are more ambiguous because fauna changes and species-dependent differences in isotopic uptake may have influenced the trends (see later discussion).

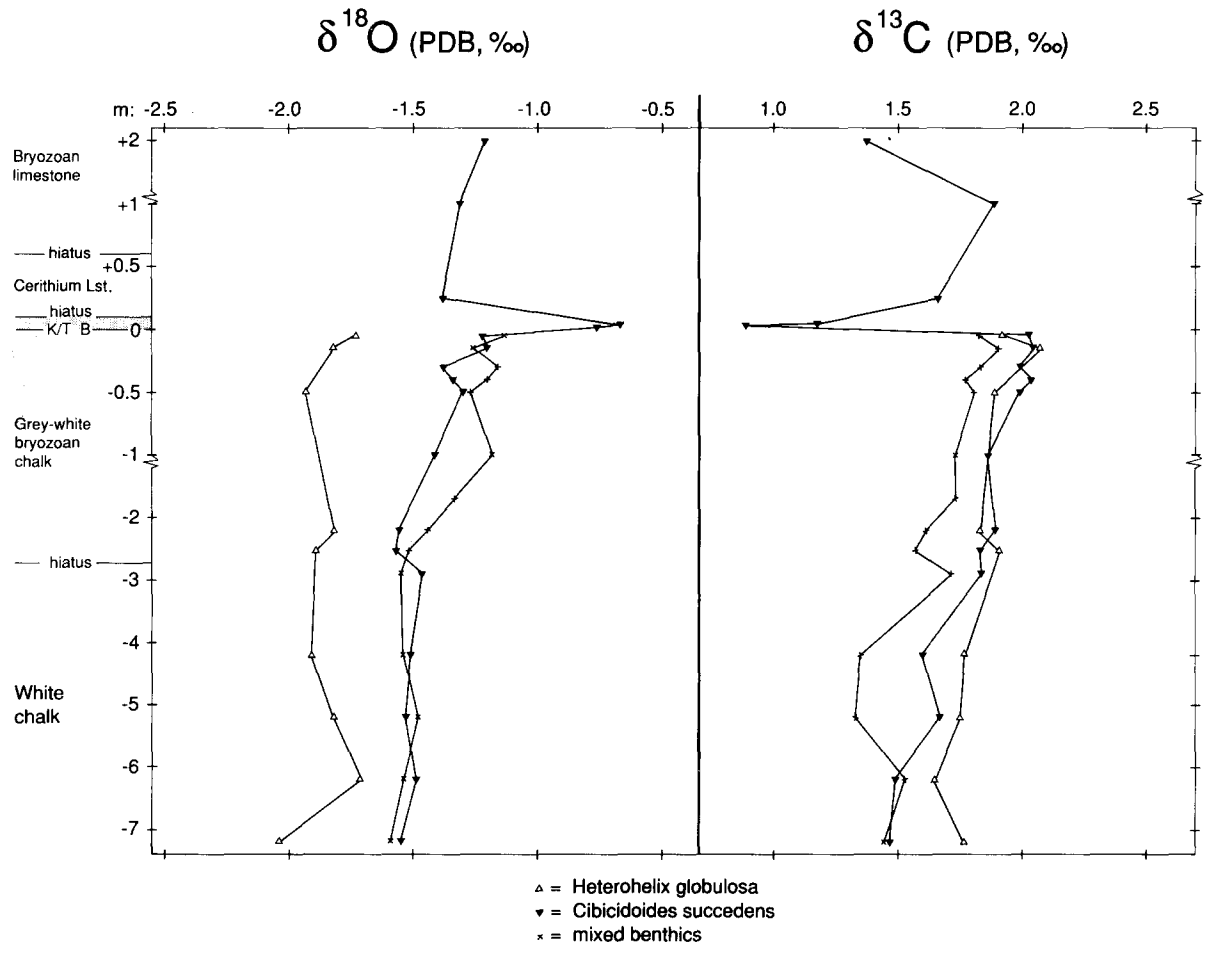

Fig. 4. Stable isotopic composition of mono- and polyspecific foraminiferal assemblages across K/T boundary section at Stevns Klint.

Differences in specimen size in *C. succedens* seems to have no significant effect on the $\delta^{18}O$ and $\delta^{13}C$ values (Fig. 6), at least when individuals smaller than 250 μm are considered. A few analyzed very large individuals of *C. succedens* (> 500 μm) show much more negative $\delta^{18}O$ values than smaller (< 250 μm) individuals from the same stratigraphic level (Table 3). As regards the difference in $\delta^{18}O$ values between very large and smaller individuals of *C. succedens*, we ascribe these to a change in feeding habits at the final stages of the life cycle for this benthic species. Possibly photosymbionts or unknown vital fractionation effects played a role in the uptake of isotopes at this stage. Present-day relatives of *C. succedens* have isotopic ratios close to equilibrium compositions (Grossman, 1987), and it is likely that the smaller *C. succedens* (< 250 μm) studied here, shows equilibrium values.

The different planktic and benthic foraminiferal species at Stevns Klint show isotopic compositions that are consistent with previously shown isotopic depth habitats of respective species (Boersma and Shackleton, 1981; Boersma and Premoli Silva, 1989). This fact together with the generally excellent shell preservation and the overall stability in the observed isotopic trends indicate that the foraminiferal $\delta^{18}O$ records generally reflect original water-mass temperature (or perhaps salinity) variations. Interpreted in terms of temperature the $\delta^{18}O$ results for *H. globulosa* imply that subsurface water temperatures at Stevns Klint were stable during

TABLE 3

Results of isotopic analyses of foraminifera from above and below the K/T boundary interval. The zero level in the profile is the base of the red K/T boundary layer

Profile depth (cm)	*C. succedens* (125–250 μm		*C. succedens* (> 500 μm)		*C. alleni* (125–250 μm)		*C. alleni* (> 500 μm)		Mixed benthics (125–250 μm)		*H. globulosa* (125–250 μm)	
	$\delta^{13}C$	$\delta^{18}O$	$\delta^{13}C$	$\delta^{18}O$	$\delta^{13}C$	$\delta^{18}O$	$\delta^{13}C$	$\delta^{18}O$	$\delta^{13}C$	$\delta^{18}O$	$\delta^{13}C$	$\delta^{18}O$
+200	+1.37	−1.21										
+100	+1.89	−1.31										
+25	+1.66	−1.38										
−20	+1.89	−1.23							+1.73	−1.11		
−30	+1.99	−1.38							+1.83	−1.16		
−40	+2.04	−1.33							+1.77	−1.20		
−50	+1.99	−1.30							+1.81	−1.27	+1.89	−1.93
−50									+1.73	−1.29		
−100	+1.86	−1.41							+1.73	−1.18		
−170									+1.73	−1.33		
−220	+1.89	−1.56	+1.84	−2.00					+1.61	−1.44	+1.83	−1.82
−220			+1.95	−2.05								
−255	+1.83	−1.57							+1.57	−1.52	+1.91	−1.89
−255									+1.51	−1.53		
−290	+1.84	−1.46							+1.72	−1.55		
−290	+1.84	−1.45										
−420	+1.60	−1.51			+1.37	−1.54	+1.37	−2.26	+1.35	−1.54	+1.77	−1.91
−420	+1.65	−1.59							+1.28	−1.55		
−520	+1.67	−1.53							+1.33	−1.48	+1.75	−1.82
−620	+1.49	−1.49							+1.53	−1.54	+1.65	−1.71
−720	+1.47	−1.55							+1.45	−1.59	+1.77	−2.04

the upper Maastrichtian at least up to 1–2 cm below the K/T boundary clay. In contrast, bottom water temperatures appear to have been constant during formation of the Maastrichtian white chalk, but decreased gradually about 1.5°C during deposition of the grey-white bryozoan chalk from 2.7 m up to the K/T boundary. With the deposition of the boundary clay, however, bottom-water temperature fell additionally about 3°C. A cooling of the water mass during deposition of the boundary clay is consistent with the increased calcite dissolution observed in the clay. Because of the early Danian hiatus (absence of Zone Pla, *P. eugubina* Zone), the post-K/T paleotemperature history cannot be determined at Stevns Klint. Our data indicate, however, that during deposition of the Cerithium Limestone, temperatures had returned to pre-K/T boundary conditions. It cannot be ruled out that the $\delta^{18}O$ variations reflect to some degree salinity rather than temperature variations, however, we presently consider this alternative as less likely.

$\delta^{13}C$ record measured in foraminifera

The $\delta^{13}C$ records of the planktic foraminifer *H. globulosa* and benthic foraminifer *C. succedens* and mixed benthic species across the upper Maastrichtian and early Danian are illustrated in Fig. 4. From 7.2 m below and up to the boundary the $\delta^{13}C$ records for both the benthic and planktic foraminifera fractions show a clearly gradual change towards 0.3–0.5‰ heavier values. Interestingly, there is a change in the surface-to-bottom $\delta^{13}C$ gradient between *H. globulosa* and *C. succedens* at the hiatus 2.7 m below the boundary. In the white chalk below the hiatus $\delta^{13}C$ values of these two species are separated by 0.2–0.4‰, whereas in the overlying grey-white chalk values for *H. globulosa* and *C. succedens* are nearly the same. These $\delta^{13}C$ changes can be readily explained by the sea-level fall observed at this interval in foraminiferal faunas. Planktic $\delta^{13}C$ values are generally heavier than benthic values because photo-

TABLE 4

Results of isotopic analyses of foraminifera across the K/T boundary interval. The zero level in the profile is the base of the red K/T boundary layer

Profile depth (cm)	*C. succedens* (125–250 μm)		*C. succedens* (125–185 μm)		*C. succedens* (185–250 μm)		Mixed benthics (125–250 μm)		*H. globulosa* (125–250 μm)		*R. rugosa* (125–250 μm)	
	$\delta^{13}C$	$\delta^{18}O$	$\delta^{13}C$	$\delta^{18}O$	$\delta^{13}C$	$\delta^{18}O$	$\delta^{13}C$	$\delta^{18}O$	$\delta^{13}C$	$\delta^{18}O$	$\delta^{13}C$	$\delta^{18}O$
+5–6							+1.87	−0.85				
+4–5							+1.88	−0.88				
+3–4							+1.71	−0.76				
+2–3	+1.20	−0.66					+1.57	−0.83				
+1.5–2	+0.89	−0.75					+1.80	−0.78				
+1.0–1.5							+2.07	−0.83				
+0.5–1.0							+2.12	−0.87				
+0.0–0.5							+1.13	−0.79				
−0.0–0.5					+2.26	−0.96	+1.96	−0.82				
−0.5–1.0			+2.20	−1.10	+2.15	−1.15	+1.92	−0.97			+2.64	−1.82
−1.0–2.0			+2.18	−1.09	+2.21	−1.09	+1.87	−1.00	+1.95	−1.72	+2.61	−1.87
−0.2	+2.06	−1.04										
−2–3			+2.17	−1.10	+2.10	−1.14	+1.94	−1.18	+2.01	−1.70	+2.64	−1.96
−3–4			+2.17	−1.16	+2.14	−1.22	+1.68	−1.06	+1.92	−1.82	+2.58	−1.93
−4–5			+2.18	−1.17	+2.24	−1.10	+1.83	−1.14	+1.92	−1.73	+2.64	−2.04
−5–6			+2.19	−1.24	+2.19	−1.15	+1.75	−1.28	+1.89	−1.80	+2.45	−2.04
−4–6	+2.03	-1.22										
−6–7			+2.24	−1.20	+2.23	−1.17	+1.96	−1.22	+2.24	−1.76	+2.64	−2.15
−7–8			+2.19	−1.17	+2.18	−1.29	+1.94	−1.14	+1.96	−1.73	+2.58	−2.10
−8–10			+2.10	−1.30	+2.18	−1.21	+1.79	−1.28	+1.84	−1.92	+2.46	−2.02
−10–12			+2.10	−0.96	+2.19	−1.17	+1.80	−1.14	+1.95	−1.80	+2.60	−2.15
−9–11	+1.99	−1.24										
−12–13							+1.76	−1.19				
−15	+2.06	−1.20	+2.14	−1.26	+2.00	−1.22	+1.91	−1.26	+2.07	−1.82	+2.61	−2.15

synthesis in the photic zone preferentially incorporates ^{12}C in organic matter and returns this carbon to the water mass during decomposition at depths (Deuser and Hunt, 1969; Kroopnick, 1974). This leads to a gradual decrease in $\delta^{13}C$ with depth. The similarity of the $\delta^{13}C$ values for the subsurface-thriving *H. globulosa* and the benthics in the uppermost Maastrichtian indicates shallow conditions and deposition probably within the photic zone. A general increase in $\delta^{13}C$ of both benthic and planktic values in the upper Maastrichtian has been observed also in deep-sea drilling cores from the Weddell Sea, Antarctica, and the Pacific Ocean (Stott and Kennett, 1989; Zachos et al., 1989), and it is likely that the positive $\delta^{13}C$ excursion at Stevns Klint reflects the same, global event (discussed later).

It is noteworthy that the mixed benthic species at Stevns Klint have generally lighter $\delta^{13}C$ values than monospecific samples of *C. succedens* (Fig. 4), a fact that probably reflects the occurrence of species with negatively fractionated $\delta^{13}C$ values in the mixed assemblages. Recent benthic foraminifera commonly show isotopic compositions that deviate somewhat from equilibrium isotopic values (Graham et al., 1981; Vincent et al., 1981; Grossman, 1987). The disequilibrium fractionation is species dependent, and therefore variations in fauna composition may have an influence on isotopic trends for mixed benthic assemblages.

Following the upper Maastrichtian increase in $\delta^{13}C$ there is a sudden major negative excursion in $\delta^{13}C$ at the K/T boundary (Figs. 4–6). This is seen in the *C. succedens* isotope profile, where a negative shift of 1.3‰ is registered at the K/T boundary (Figs. 4 and 6). Also the mixed benthic profile shows a negative shift, however, the trend is more complex probably due to fauna changes

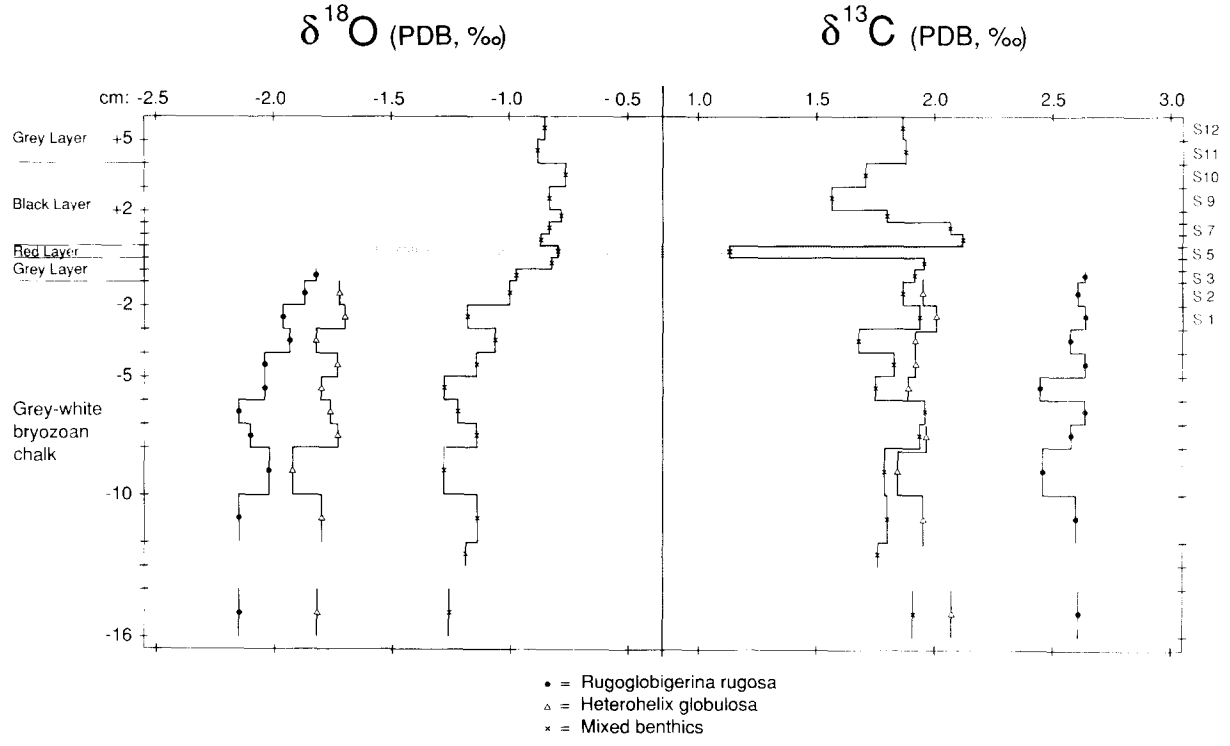

Fig. 5. Stable isotopic composition of mono- and polyspecific foraminiferal assemblages in high-resolution profile spanning the interval immediately below and across the K/T boundary clay at Stevns Klint.

(Fig. 5). In the red layer at the base of the boundary clay $\delta^{13}C$ values for mixed benthics drop nearly 1‰, but return to Maastrichtian values already in the overlying black clay. Below the K/T boundary $\delta^{13}C$ values for both planktic and benthic foraminifera are stable from 16 cm below up to the red layer (Figs. 5–6). Noteworthy in this interval are the much heavier $\delta^{13}C$ values in the *R. rugosa* assemblages compared with *H. globulosa* and mixed benthics, which show similar values. These $\delta^{13}C$ data indicate that biological productivity was high in the surface waters and that there was a surface-to-bottom $\delta^{13}C$ gradient in the water mass until the very end of the Cretaceous. The similarity in $\delta^{13}C$ values for *H. globulosa* and mixed benthics indicates that water depth was still relatively shallow.

A prominent negative carbon isotope anomaly at the K/T boundary has previously been found at many sites (Hsü et al., 1982; Perch-Nielsen et al., 1982; Zachos and Arthur, 1986; Keller and Lindinger, 1989; Zachos et al., 1989; Barrera and Keller, 1990). In general, this isotopic anomaly is recorded in planktic foraminifera or coccolith ooze, but not in benthic foraminifera, suggesting that only the $\delta^{13}C$ of the upper water mass was affected. The K/T boundary negative $\delta^{13}C$ shift is commonly attributed to large-scale reduction of biological productivity in the euphotic zone, which would disrupt the biological carbon pump, resulting in a diminished surface-to-bottom $\delta^{13}C$ gradient (Hsü et al., 1982; Zachos et al., 1989). At Stevns Klint the absence of planktic foraminifera in the boundary clay prevents direct determination of the $\delta^{13}C$ composition of K/T boundary surface waters. Because of the shallow water depth at this site, however, the benthic foraminiferal $\delta^{13}C$ values are indicative of isotopic trends in the lower part of the euphotic zone. Therefore the benthic negative $\delta^{13}C$ anomaly at this site most likely reflects the same isotope anomaly that previously has been measured in planktic organisms at other K/T boundary sites.

There is another possibility, namely that the

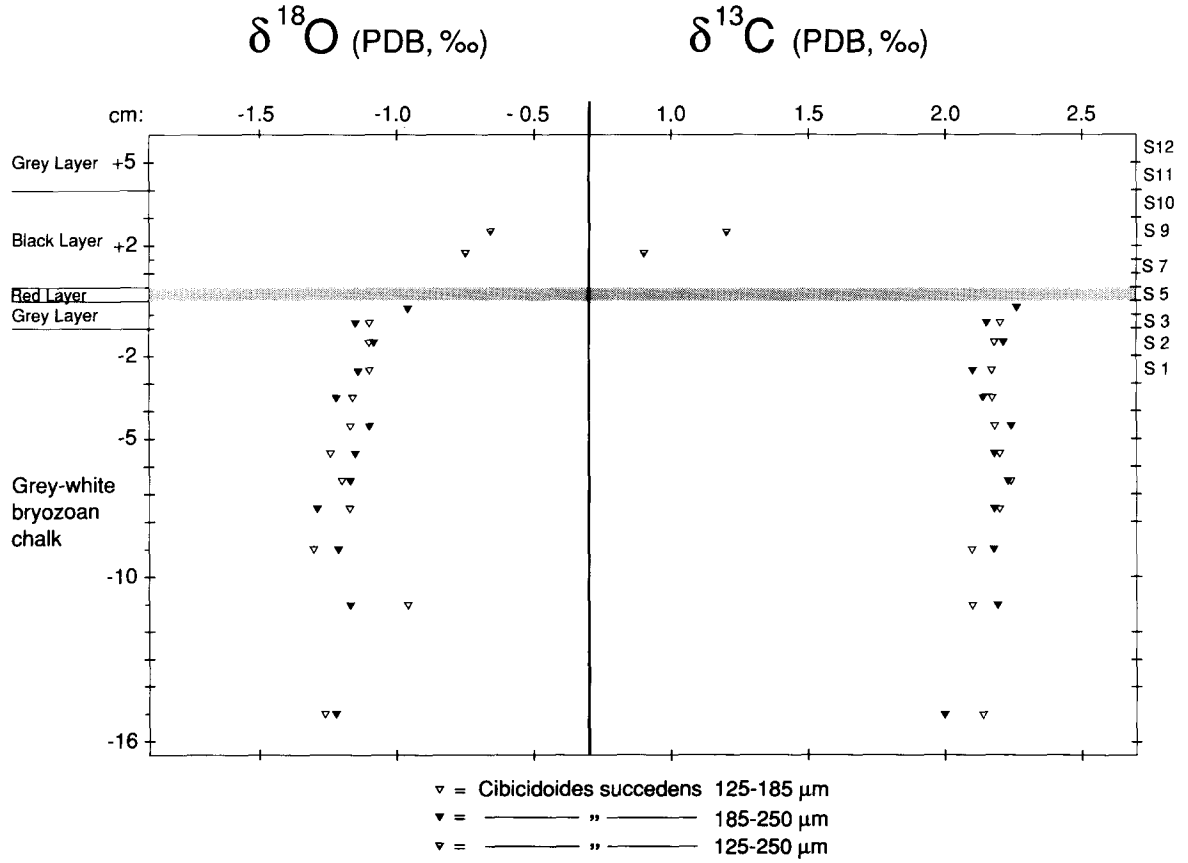

Fig. 6. Stable isotopic composition of benthic foraminifera *C. succedens* in high-resolution profile spanning the interval immediately below and across the K/T boundary clay at Stevns Klint.

negative $\delta^{13}C$ anomaly at Stevns Klint is primarily related to extensive sea-floor microbial activity and anoxic conditions. Lazar and Erez (1990) have recently shown that because of kinetic fractionation processes the $\delta^{13}C$ values in calcite that forms in microbial mats become very negative. Abundant pyrite, chalcophile trace element enrichments and extremely negative $\delta^{34}S$ values measured in the Fish Clay have previously been interpreted as representing evidence for flourishing microbial activity and anoxic conditions on the sea floor in connection with the K/T boundary event (Schmitz, 1988). A microbially induced negative $\delta^{13}C$ anomaly appears less likely, however, when considering that the analyzed benthic foraminifera at Stevns Klint probably did not live in the anoxic Fish Clay basins, but were transported there from the oxygenated interbasinal bioherms.

Bulk-rock isotopic record

Whole-rock or "fine fraction" isotopic trends have previously been studied at Stevns Klint by Romein and Smit (1981) and Kaminski and Malmgren (1989). The value of such isotopic data is limited, because variations in the relative amounts of different components with different isotopic compositions may to a large extent determine the measured isotopic trends (e.g. Paull and Thierstein, 1987). Moreover, if only whole-rock data are considered, it is very difficult to assess to what degree isotopic signals are original or diagenetically modified.

From 7.2 m below up to immediately below the K/T boundary both $\delta^{18}O$ and $\delta^{13}C$ whole-rock values are stable (Fig. 7). At the boundary, there is a dramatic positive shift in $\delta^{18}O$, that is followed

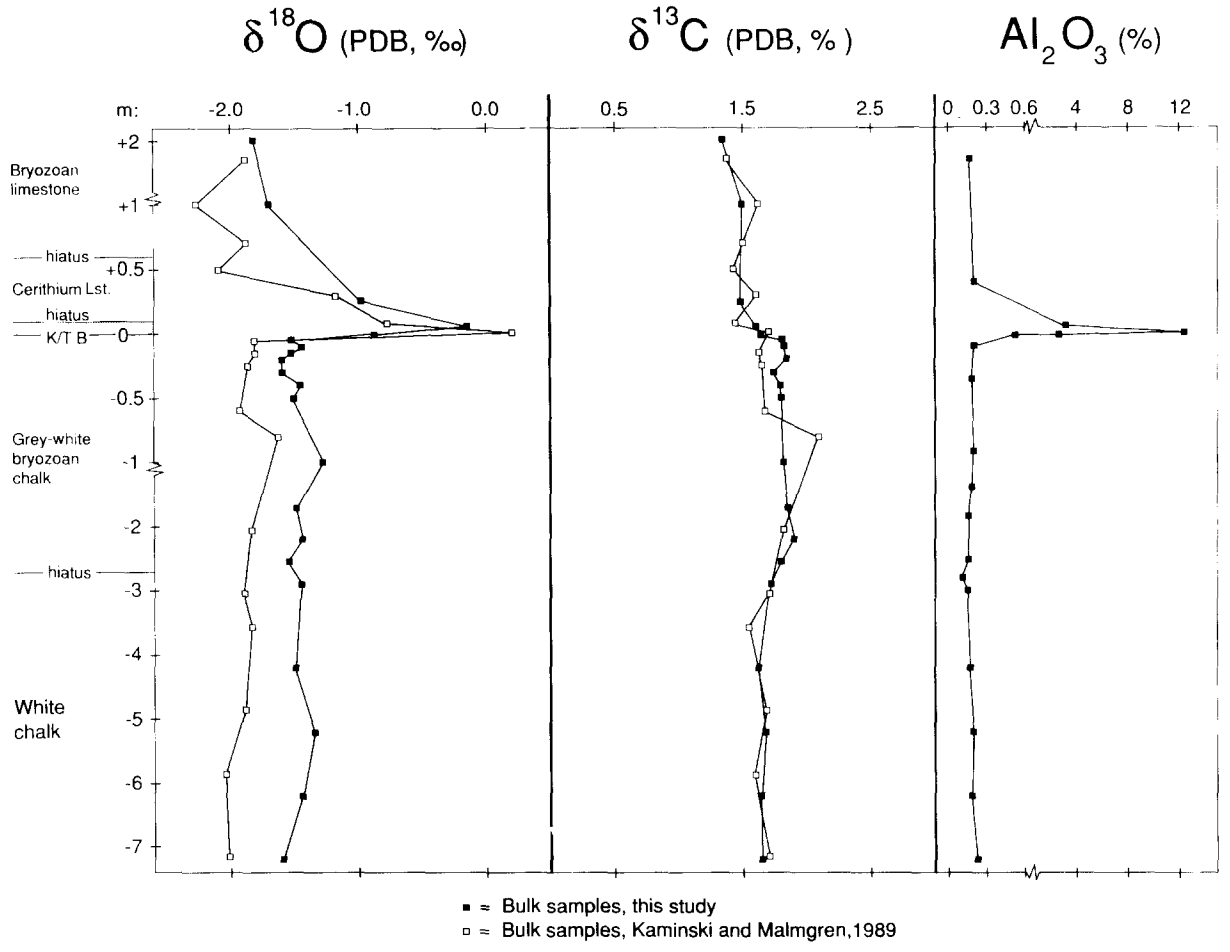

Fig. 7. Stable isotopes and Al_2O_3 content in bulk samples across the K/T boundary section at Stevns Klint. Alumina-oxide analyses were performed on bulk samples with Inductively Coupled Plasma-Optical Emission Spectroscopy; for analytical details, see Schmitz (1987).

by a return to more negative values in the Cerithium Limestone. One meter above the boundary $\delta^{18}O$ values are somewhat more negative than in the Maastrichtian. The $\delta^{13}C$ values show a small negative shift at the boundary and Danian values remain more negative than Maastrichtian values. In general, our results are similar to those obtained by Kaminski and Malmgren (1989), however, our $\delta^{18}O$ values are constantly about 0.3–0.4‰ heavier than theirs, a fact that probably is due to differences in calibration of the analyses.

A high-resolution profile across the K/T boundary interval is shown in Fig. 8. The most notable result here is the gradual increase in $\delta^{18}O$ values in a 4-cm thick interval immediately below the red K/T boundary layer. The calcite content of the red layer is too low to give good isotopic values. Above the red layer the $\delta^{18}O$ values first return to those measured about 5 cm below the red layer. Thereafter $\delta^{18}O$ values increase reaching a maximum 6 cm above the red layer. The $\delta^{13}C$ values show a very stable trend in the dm-thick interval just below the boundary clay. Only in the 0.5 cm thick interval immediately below the red layer do the $\delta^{13}C$ values fall. Minimum $\delta^{13}C$ values are measured about 2–3 cm above the red layer, where the $\delta^{13}C$ values are about 0.7‰ lighter than in the uppermost Maastrichtian chalk (Figs. 7–8).

Our bulk-rock isotopic profile across the boundary clay registers the same positive $\delta^{18}O$ shift as

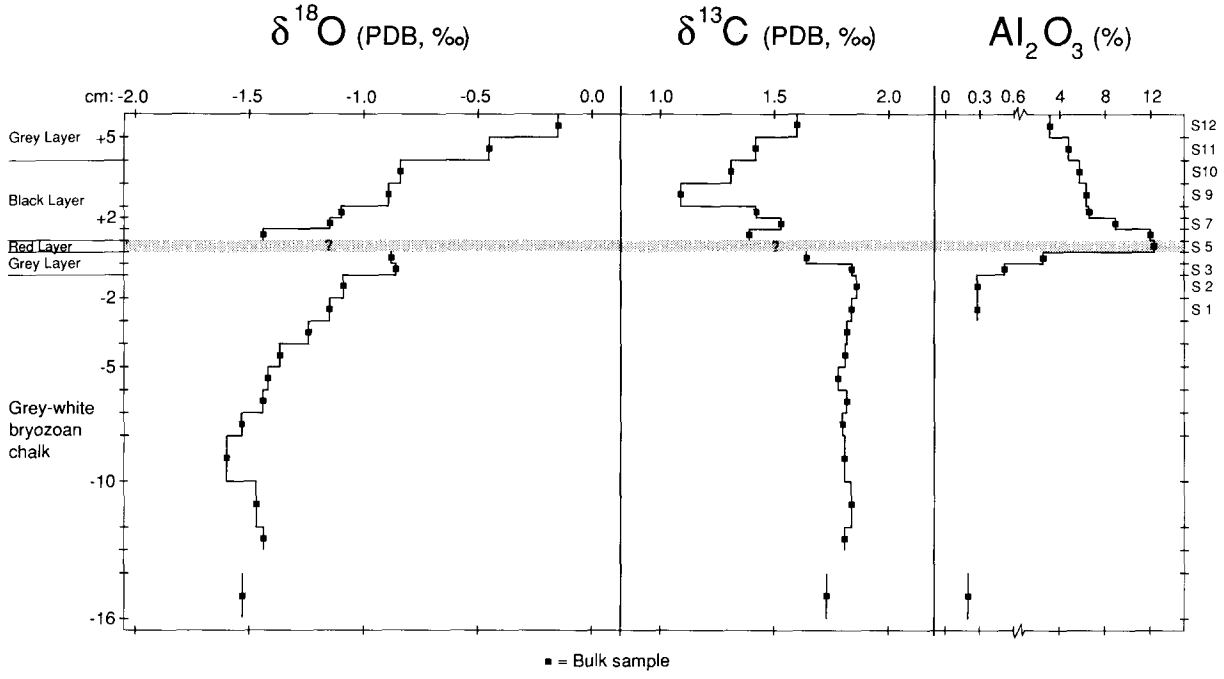

Fig. 8. Stable isotopic composition of bulk samples in high-resolution profile spanning the interval immediately below and across the K/T boundary clay at Stevns Klint. For information on alumina-oxide analyses, see caption for Fig. 7.

previously reported by Romein and Smit (1981) and Kaminski and Malmgren (1989), however, the detailed development of this shift appears different in our study. For example, in the two previous studies the maximum positive $\delta^{18}O$ shift is in the lower part of the boundary clay, whereas we measure a maximum in the upper part of the boundary clay. The gradual increase in $\delta^{18}O$ immediately below the boundary is not apparent in the study by Romein and Smit (1981); however, the data by Malmgren and Kaminski (1989) show this decline. The different results obtained may reflect different sample preparation techniques. Whereas we analyzed finely ground whole-rock samples, Romein and Smit (1981) analyzed fine-fraction material recovered by water-column settling and decantation, and Kaminski and Malmgren (1989) analyzed chalk fragments in the size-range 125–250 μm.

It is notable that in some of the sublayers of the K/T boundary clay $\delta^{18}O$ values are as much as 0.7‰ heavier in bulk samples than in benthic foraminifera. If a temperature change is responsible for this shift, this would imply that surface waters became colder than the bottom waters during formation of the boundary clay, in support of the global darkness scenario by Alvarez et al. (1980). There are some reasons, however, to doubt that bulk-sample isotopic records primarily reflect temperature variations. For example, the bulk-sample $\delta^{18}O$ values increase gradually across the 4-cm interval below the K/T boundary, whereas over the same interval, the surface-dweller *R. rugosa* and the mid-depth dweller *H. globulosa* show relatively stable $\delta^{18}O$ trends. While picking the foraminifera for isotopic analyses in the 5 cm interval immediately below the boundary clay, we noticed that planktic foraminifera become increasingly more rare towards the boundary. We noticed also that benthic foraminifera become increasingly corroded as we approached the boundary clay. Because the gradual pre-K/T boundary $\delta^{18}O$ positive shift occurs parallel to increased calcite dissolution, these trends may be related. With increasing calcite dissolution particles with a high surface-to-mass ratio, such as planktic nannofossil calcite, will be preferentially dissolved. Massive calcite formed by bryozoa and other benthic ani-

mals will resist dissolution to a much higher degree, leading to a positive shift in $\delta^{18}O$. In the upper part of the boundary clay, where $\delta^{18}O$ values are heavier in the bulk rock even than in the benthic foraminifera, selective dissolution of different kinds of calcite cannot explain the positive shift. Another unknown process must also have played a role. The bulk-sample $\delta^{18}O$ positive shift is not likely to be due to isotopic reequilibration with meteoric water during epigenesis and weathering, because this would with a high probability have shifted the $\delta^{18}O$ values in the opposite direction.

The calcite dissolution in the 3–4 cm thick interval below the boundary may have taken place in the water column and on the sea-floor shortly before the deposition of the spherule-rich red layer. The interval is characterized also by the occurrence of abundant Mn-micronodules, and common black (possibly Mn-oxide) staining of bryozoa remains. The abundance of Mn-nodules in the layer is consistent with formation during turbulent, corrosive and well-oxygenated bottom-water conditions. Thus, anomalously turbulent conditions preceded the stagnant conditions that occurred during formation of the anoxic K/T boundary clay (Schmitz, 1988).

Discussion

Although a multitude of stable isotopic studies of the K/T boundary transition worldwide have been published, the timing and magnitude of productivity-induced $\delta^{13}C$ changes are still controversial, and $\delta^{18}O$ temperature trends are enigmatic with many studies providing contradictory results. This is partly because most K/T boundary isotopic studies are based on bulk-rock or fine fraction carbonate, of which each may carry multiple biogenic components (e.g. benthic and planktic foraminifera, nannofossils) and nonbiogenic calcite. The isotopic composition of such carbonate is determined by many factors, such as variations in relative abundance of different types of calcite, diagenetic alteration, dissolution and isotopic fractionation effects. Thus, many published records are difficult, if not impossible, to interpret. Moreover, precise correlation of these records is nearly impossible, because most K/T boundary sections have been shown to be temporally incomplete with hiatuses, non-deposition, or condensed intervals (MacLeod and Keller, 1991a, b). Despite these difficulties, the following $\delta^{13}C$ and $\delta^{18}O$ history has emerged.

Most studies agree that a negative $\delta^{13}C$ shift occurs at or near the K/T boundary associated with a reduced surface-to-deep $\delta^{13}C$ gradient variously estimated to have lasted between 100–500 kyr (Keller and Lindinger, 1989; Stott and Kennett, 1989; Zachos et al., 1989; Barrera and Keller, 1990). As discussed earlier this $\delta^{13}C$ shift is generally interpreted as a disruption of the biological carbon pump due to major reduction in the primary productivity of the oceans. Although in most deep-sea sections this $\delta^{13}C$ shift appears to be instantaneous and coincident with the Ir anomaly that often marks the K/T boundary, this appears to be an artifact of an incomplete chronostratigraphic record (MacLeod and Keller, 1991a, b). In more complete, high sedimentation records the $\delta^{13}C$ shift occurs gradually and after the Ir anomaly (Stott and Kennett, 1989; Barrera and Keller, 1990). Owing to the poor carbonate preservation in the boundary interval at Stevns Klint, the detailed post-impact carbon distribution in the water column at this site cannot be determined. The benthic foraminifera, however, show reduced $\delta^{13}C$ values already in the lower part of the K/T boundary clay, suggesting that the negative $\delta^{13}C$ shift at this site occurred relatively soon after the bolide impact event. One problem, however, is that the Fish Clay most likely represents a very condensed sediment, and a significant amount of time may have passed between the formation of the spherule-rich red layer and the black clay some centimeters higher up (Schmitz, 1990b).

A positive $\delta^{13}C$ shift in benthic and planktic isotope records has been observed beginning about 200 kyr below the K/T boundary, preceeding the negative $\delta^{13}C$ shift, at DSDP Sites 577 and 690 (Stott and Kennett, 1989; Zachos et al., 1989). At Stevns Klint this positive carbon isotopic excursion is also observed, and similarly to the previously established isotopic records, the planktic and the benthic values converge towards the boundary, because of a higher gradient in the benthic shift. The late Maastrichtian positive $\delta^{13}C$ shift has been

variously related to a change in the $\delta^{13}C$ composition of the oceans, a change in deep-water circulation or reduced carbon flux during a rise in sea level (Stott and Kennett, 1989; Zachos et al., 1989). The latter interpretation can be ruled out because our planktic and benthic foraminiferal studies at Stevns Klint show that the positive $\delta^{13}C$ shift evolves across both shallowing and deepening successions, suggesting lack of relationship with sea-level.

The paleotemperature record across the K/T boundary transition is more difficult to interpret because $\delta^{18}O$ values are more easily affected by diagenetic alteration than the $\delta^{13}C$ values. Notwithstanding these difficulties, for instance, Zachos and Arthur (1986) concluded that there were no outstanding changes in either bottom or surface water temperatures across the K/T boundary. Barrera and Keller (1990), however, interpreted a 3‰ negative $\delta^{18}O$ shift in both planktic and benthic foraminifera at the mid-neritic Brazos River section as the result of both warmer temperatures and a change in salinity. Smit (1990) observed a similar negative shift in bulk carbonate of the Agost and Caravaca sections of southern Spain and interpreted it as a 8°C surface warming. In contrast, at the outer neritic section of El Kef bottom-water cooling of possibly 4–5°C is indicated after the K/T boundary (Keller and Lindinger, 1989). Cooler bottom-water temperatures of about 1.5°C are also indicated at Stevns Klint beginning well below the K/T boundary and associated with the sea level fall observed in foraminiferal assemblages. A further cooling of 3°C occurs during formation of the boundary clay. Bottom-water temperatures increase in Zone P1a (*P. eugubina*) at El Kef and in the Cerithium Limestone at Stevns Klint. These isotopic records indicate that the paleotemperature history of the oceans was complex and unstable across the K/T boundary, probably as a result of changing oceanic circulation patterns (Schmitz, 1990a; Schmitz et al., 1991).

Sea-level changes, and the frequently associated stratigraphic unconformities have received little attention in K/T boundary scenarios, which primarily focus on Ir anomalies, shocked quartz and species extinctions. Yet these changes are critical in interpreting both the nature and rate of environmental changes as well as species extinctions that characterize the K/T transition (Keller, 1988a, 1989a). There is ample evidence for K/T boundary sea-level fluctuations (Officer et al., 1987; Hallam, 1987; MacLeod and Keller, 1991a, b), and the most detailed records are available from outer slope and shelf regions such as El Kef, Tunisia and Agost, Spain. At these sites sea level shallows from upper slope to shelf depth during the latest Maastrichtian and then rises again during deposition of the K/T boundary black clay and subsequent early Danian deposits (Brinkhuis and Zachariasse, 1988; Keller, 1988a, in press; Canudo et al., 1991; MacLeod and Keller, 1991a, b). In the eastern Tethys (e.g. Negev of Israel and southern Egypt) alternating shallowing and deepening seas associated with hiatuses characterize K/T boundary and early Paleocene deposits (Keller et al., 1990; Schmitz, unpubl. results). In Alabama a regression culminates near the end of the Maastrichtian and is followed by a transgression into the Danian (Jones et al., 1987; Donovan et al., 1988).

In this study we observed that the K/T boundary transition at Stevns Klint also occurred during a period of prominent sea level instability. Planktic and benthic foraminifera, as well as ^{13}C isotopes indicate that a sea level fall marked by an omission surface occurred between deposition of the white chalk and overlying grey-white chalk 2.7 m below the K/T boundary (see also Ekdale and Bromley, 1984). We estimate that sea-level fell about 50–100 m, which implies that, if a global feature is registered this is one of the most dramatic sea-level falls that took place during the Phanerozoic (cf. with sea-level curve of Haq et al., 1987). About 40 cm below the K/T boundary and into the early Danian, sea-level began to rise as noted by an influx of the open marine surface dweller *Rugoglobigerina rugosa*, decline in the shallow water taxa *Guembelitria* and reappearance of deeper neritic benthic taxa. The two hiatuses noted near the top of the Fish Clay (*P. eugubina*, P1a Zone) and at the base of the Cerithium Limestone (Zones P1b–P1c) probably represent short sea-level falls during generally transgressive early Danian seas as also observed in sections in Spain (Canudo et al., 1991), eastern Tethys (Keller et al., 1990) and Brazos

River, Texas (Keller, 1989a; MacLeod and Keller 1991a, b). The widespread nature of these hiatuses suggest global eustatic changes, which probably took place along with major climatic and oceanic circulation changes.

It appears that the K/T boundary transition at Stevns Klint, as well as in the best K/T boundary sections worldwide, is characterized by a 100–500 kyr long period of oceanic instability. At Stevns Klint important bottom-water temperature and major rapid sea-level changes are registered from 2.7 m below to 0.6 m above the boundary. At many sites worldwide similar gradual changes have been observed across the K/T boundary: Sea-level changes, hiatus formation, prolonged suppression of primary productivity, gradual extinction of foraminifera and nannofossils, and long periods of clay and marl deposition in marine environments where chalks used to form (see references in introduction). This long-term oceanic instability, beginning largely during the latest Maastrichtian, seems impossible to explain by a single bolide impact at K/T boundary time and could, in fact, represent a mere temporal coincidence. Scenarios which favor a terrestrial mechanism for these long-term changes invoke volcanism as the primary driving force for sea-level and temperature changes and envision a volcanic origin for iridium and shocked quartz accumulations (Officer et al., 1987). Current extraterrestrial impact scenarios attempt to explain these long-term changes by proposing multiple impacts (Hut et al., 1991). An alternative scenario discussed by Schmitz et al. (1991) suggests that the K/T boundary bolide impact was merely a reflection of an order-of-magnitude larger astronomical event, causing long-term gravitational instability in the solar system. This event may have led to perturbations in earth rotation, oceanic eustasy and circulation patterns. Repeated destruction of the oceanic trophic structure may have killed all those plankton species that could not adapt to constantly changing environmental conditions. It is notable that sea-level and bottom water temperature changes at Stevns Klint occur over approximately the same stratigraphic interval in which supposed extraterrestrial amino acids have been found (this study; Zhao and Bada, 1989). Zahnle and Grinspoon (1990) suggest that the amino acids derive from a dust cloud accompanying a giant comet that passed nearby the Earth. In their scenario the K/T boundary impactor represents merely a fragment of this comet. However, very little is known about amino acids in fossil sediments, and it cannot be ruled out that the amino acids simply diffused out from the boundary clay. Although long-term oceanic instability coincides with an extraterrestrial bolide impact event at the K/T boundary, the relation between these two events is still obscure, and more stratigraphic and geochemical data is needed in order to disentangle whether there possibly is a connection.

Acknowledgements

This study was supported by grants from the Erna and Victor Hasselblad Foundation, Swedish Natural Science Research Council and Magnus Bergvall Foundation. We are grateful to O. Gustafsson for isotopic analyses, to S. Nemethy and U. Schwarz for field assistance, to T. Alavi, T. Andinsson and R. Svensson for laboratory work, and to M. Eliasson for drawings. Comments by F. Surlyk, K. von Salis Perch-Nielsen and an anonymous referee improved the paper.

References

Alvarez, L.W., Alvarez, W., Asaro, F. and Michel, H.V., 1980. Extraterrestrial cause for the Cretaceous–Tertiary extinction. Science, 208: 1095–1108.

Alvarez, W., Alvarez, L.W., Asaro, F. and Michel, H.V., 1984a. The end of the Cretaceous: Sharp boundary or gradual transition? Science, 223: 1183–1186.

Alvarez, W., Kauffman, E.G., Surlyk, F., Alvarez, L.W., Asaro, F. and Michel, H.V., 1984b. Impact theory of mass extinctions and the invertebrate fossil record. Science, 223: 1135–1141.

Barrera, E. and Huber, B.T., 1990. Evolution of Antarctic Water during the Maastrichtian: Foraminifer oxygen and carbon isotope ratios, Leg 113. ODP Sci. Res., 113: 813–827.

Barrera, E. and Keller, G., 1990. Stable isotope evidence for gradual environmental changes and species survivorship across the Cretaceous/Tertiary boundary. Paleoceanography, 5: 867–890.

Berggren, W.A., Kent, D.V. and Flynn, J.J., 1985. Paleogene geochronology and chronostratigraphy. Mem. Geol. Soc. London, 10: 141–195.

Birkelund, T. and Bromley, R.G. (Editors), 1979. Cretaceous–Tertiary boundary events, I. The Maastrichtian and Danian of Denmark. Univ. Copenhagen, pp. 1–210.

Boersma, A. and Premoli Silva, I., 1989. Atlantic Paleogene

biserial heterohelicid foraminifera and oxygen minima. Paleoceanography, 4: 271–286.

Boersma, A. and Shackleton, N.J., 1981. Oxygen and carbon isotope variations and planktonic foraminiferal depth habitats: Late Cretaceous to Paleocene, Central Pacific, DSDP Sites 463 and 465, Leg 63. In: Init. Rep. DSDP, 63: 513–526.

Boersma, A., Shackleton, N., Hall, M. and Given, Q., 1979. Carbon and oxygen isotope records at DSDP Site 384 (North Atlantic) and some Paleocene paleotemperatures and carbon isotope variation in the Atlantic Ocean. In: Init. Rep. DSDP, 43: 695–717.

Brinkhuis, W. and Zachariasse, W.J., 1988. Dinoflagellate cysts, sea level changes and planktonic foraminifers across the Cretaceous-Tertiary boundary at El Haria, northwest Tunisia. Mar. Micropaleontol., 13: 153–191.

Bromley, R.G., 1979. Chalk and bryozoan limestone: Facies, sediments and depositional environments. In: T. Birkelund and R.G. Bromley (Editors), Cretaceous–Tertiary boundary events, I. The Maastrichtian and Danian of Denmark. Univ. Copenhagen, pp. 16–33.

Canudo, I., Keller, G. and Molina, E., 1991. K/T boundary extinction pattern and faunal turnover at Agost and Caravaca, SE Spain. Mar. Micropaleontol., 17: 319–341.

Christensen, L., Fregerslev, S., Simonsen, A. and Thiede, J., 1973. Sedimentology and depositional environment of lower Danian Fish Clay from Stevns Klint, Denmark. Bull. Geol. Soc. Den., 22: 193–212.

Deuser, W.G. and Hunt, J.M., 1969. Stable isotope ratios of dissolved inorganic carbon in the Atlantic. Deep-Sea Res., 16: 221–225.

D'Hondt, S. and Keller, G., 1991. Some patterns of planktic foraminiferal assemblage turnover at the Cretaceous–Tertiary boundary. Mar. Micropaleontol., 17: 77–118.

Donovan, A.D., Baum, G.R., Blechschmidt, G.L., Loutit, T.S., Pflum, C.E. and Vail, P.R., 1988. Sequence stratigraphic setting of the Cretaceous–Tertiary boundary in Central Alabama. SEPM Spec. Publ., 42: 300–307.

Douglas, R.G. and Savin, S.M., 1978. Oxygen isotope evidence for depth stratification of Tertiary and Cretaceous planktic foraminifera. Mar. Micropaleontol., 3: 175–196.

Ekdale, A.A. and Bromley, R.G., 1984. Sedimentology and ichnology of the Cretaceous–Tertiary boundary in Denmark: Implications for the causes of the terminal Cretaceous extinction. J. Sediment. Petrol., 54: 681–703.

Elliot, W.C., Aronsson, J.L., Millard Jr. H.T. and Gierlowski-Kordesch, E., 1989. The origin of the clay minerals at the Cretaceous/Tertiary boundary in Denmark. Geol. Soc. Am. Bull., 101: 702–710.

Graham, D.W., Corliss, B.H., Bender, M.L. and Keigwin, L.D., 1981. Carbon and oxygen isotopic disequilibria of recent deep-sea benthic foraminifera. Mar. Micropaleontol., 6: 483–497.

Grossman, E., 1987. Stable isotopes in modern benthic foraminifera: A study of vital effect. J. Foraminiferal Res., 17: 48–61.

Håkansson, E., Bromley, R. and Perch-Nielsen, K., 1974. Maastrichtian chalk of northwest Europe—a pelagic shelf sediment. In: K.J. Hsü and M.C. Jenkyns (Editors), Pelagic Sediments: On the Land and Under the Sea. IAS Spec. Publ., 1: 211–234.

Hallam, A., 1987. End-Cretaceous mass extinction event: Argument for terrestrial causation. Science, 238: 1237–1242.

Hansen, J.M., 1978. A new dinoflagellate zone at the Maastrichtian/Danian boundary in Denmark. Dan. Geol. Unders. Årb. 1978, pp. 131–140.

Haq, B.U., Hardenbol, J. and Vail, P.R., 1987. Chronology of fluctuating sea levels since the Triassic. Science, 235: 1156–1166.

Hsü, K.J., He, Q., McKenzie, J.A., Weissert, H., Perch-Nielsen, K., Oberhänsli, H., Kelts, K., LaBrecque, J., Tauxe, L., Krähenbühl, U., Percival Jr., S.F., Wright, R., Karpoff, A.M., Petersen, N., Tucker, P., Poore, R.Z., Gombos, A.M., Pisciotto, K., Carman Jr., M.F. and Schreiber, E., 1982. Mass mortality and its environmental and evolutionary consequences. Science, 216: 249–256.

*Hultberg, S.U. and Malmgren, B.A., 1986. Dinoflagellate and planktonic foraminiferal paleobathymetrical indices in the boreal uppermost Cretaceous. Micropaleontology, 32: 316–323.

Hultberg, S.U. and Malmgren, B.A., 1987. Quantitative biostratigraphy based on Late Maastrichtian dinoflagellates and planktonic foraminifera from southern Scandinavia. Cretaceous Res., 8: 211–228.

Hut, P., Shoemaker, E.M., Alvarez, W. and Montanari, A., 1991. Astronomical mechanisms and geologic evidence for multiple impacts on Earth. In: Abstr. 22nd Lunar Planet. Sci. Conf., Houston, Tex.

Jiang, M.J. and Gartner, S., 1986. Calcareous nannofossil succession across the Cretaceous/Tertiary boundary in east-central Texas. Micropaleontology, 32: 232–255.

Jones, D.S., Mueller, P.A., Bryan, J.R., Dobson, J.P., Channell, J.E.T., Zachos, J.C. and Arthur, M.A., 1987. Biotic, geochemical, and paleomagnetic changes across the Cretaceous/Tertiary boundary at Braggs, Alabama. Geology, 15: 311–315.

Kaminski, M.A. and Malmgren, B.A., 1989. Stable isotope and trace element stratigraphy across the Cretaceous/Tertiary boundary in Denmark. Geol. Fören. Stockh. Förh., 111: 305–312.

Kastner, M., Asaro, F., Michel, H.V., Alvarez, W. and Alvarez, L.W., 1984. The precursor of the Cretaceous–Tertiary boundary clays at Stevns Klint, Denmark, and DSDP Hole 465A. Science, 226: 137–143.

Keller, G., 1985. Depth stratification of planktonic foraminifera in the Miocene Ocean. Geol. Soc. Am. Mem., 163: 177–194.

Keller, G., 1988a. Extinction, survivorship and evolution of planktic foraminifera across the Cretaceous/Tertiary boundary at El Kef, Tunisia. Mar. Micropaleontol., 13: 239–263.

Keller, G., 1988b. Biotic turnover in benthic foraminifera across the Cretaceous/Tertiary boundary at El Kef, Tunisia. Palaeogeogr., Palaeoclimatol., Palaeoecol., 66: 153–171.

Keller, G., 1989a. Extended Cretaceous/Tertiary boundary extinctions and delayed population change in planktonic foraminifer from Brazos River, Texas. Paleoceanography, 4: 287–332.

Keller, G., 1989b. Extended period of extinctions across the Cretaceous/Tertiary boundary in planktonic foraminifera of continental shelf sections: Implications for impact and volcanism theories. Geol. Soc. Am. Bull., 101: 1408–1419.

Keller, G., in press. Paleoecological response of Tethyan benthic

foraminifera to the Cretaceous/Tertiary transition. Proc. 4th Int. Symp. Benthic Foraminifera, Sendai, 1990. Elsevier.

Keller, G. and Lindinger, M., 1989. Stable isotope, TOC and $CaCO_3$ records across the Cretaceous/Tertiary boundary at El Kef, Tunisia. Palaeogeogr., Palaeoclimatol., Palaeoecol., 73: 243–265.

Keller, G., Benjamini, C., Magaritz, M. and Moshkovitz, S., 1990. Faunal, erosional, and $CaCO_3$ events in the early Tertiary eastern Tethys. Geol. Soc. Am. Spec. Pap., 247: 471–480.

Keller, G., MacLeod, N. and Barrera, E., 1992. Eocene–Oligocene faunal turnover in planktic foraminifera and Antarctic glaciation. In: D. Prothero and W.A. Berggren (Editors), The Eocene–Oligocene Transition. Princeton Univ. Press.

Kent, D.V. and Gradstein, F.M., 1985. A Cretaceous and Jurassic geochronology. Geol. Soc. Am. Bull., 96: 1419–1427.

Kroon, D. and Nederbragt, A.J., 1990. Ecology and paleoecology of triserial planktic foraminifera. Mar. Micropaleontol., 16: 25–38.

Kroopnick, P., 1974. The dissolved O_2-CO_2-^{13}C system in the eastern equatorial Pacific. Deep-Sea Res., 21: 211–277.

Kyte, F.T., Zhou, Z. and Wasson, J.T., 1980. Siderophile-enriched sediments from the Cretaceous–Tertiary boundary. Nature, 288: 651–656.

Lazar, B. and Erez, J., 1990. Extreme ^{13}C depletions in seawater derived brines and their implications for the past geochemical carbon cycle. Geology, 18: 1191–1194.

MacLeod, N. and Keller, G., 1991a. Hiatus distribution and mass extinctions at the Cretaceous/Tertiary boundary. Geology, 19: 497–501.

MacLeod, N. and Keller, G., 1991b. How complete are Cretaceous/Tertiary boundary sections? A chronostratigraphic estimate based on graphic correlation. Geol. Soc. Am. Bull., 103: 1439–1457.

Malmgren, B.A., 1981. Biostratigraphy of planktic foraminifera from the Maastrichtian white chalk of Sweden. Geol. Fören. Stockh. Förh., 103: 357–375.

Officer, C.B., Hallam, A., Drake, C.L. and Devine, J.D., 1987. Late Cretaceous and paroxysmal Cretaceous/Tertiary extinctions. Nature, 326: 143–149.

Paull, G.K. and Thierstein, H.R., 1987. Stable isotope fractionation among particles in Quaternary coccolith-sized deep-sea sediments. Paleoceanography, 2: 423–429.

Perch-Nielsen, K., McKenzie, J. and He, Q., 1982. Biostratigraphy and isotope stratigraphy and the "catastrophic" extinction of calcareous nannoplankton at the Cretaceous/Tertiary boundary. Geol. Soc. Am. Spec. Pap., 190: 353–371.

Pospichal, J.J. and Wise Jr., S.W., 1990. Calcareous nannofossils across the K/T boundary, ODP Hole 690C, Maud Rise, Weddell Sea. In: Proc. ODP Sci. Res., 113: 515–531.

Rampino, M.R. and Reynolds, R.G., 1983. Clay mineralogy of the Cretaceous–Tertiary boundary clay. Science, 219: 495–498.

Rocchia, R., Renard, M., Boclet, D. and Bonte P., 1984. Essai d'évaluation de la durée de la transition Crétacé/Tertiaire par l'évolution de l'anomalie en iridium; implications dans la recherche de la cause de la crise biologique. Bull. Soc. Géol. Fr., 6: 1193–1202.

Rocchia, R., Boclet, D., Bonte, P., Devineau, J., Jehanno, C. and Renard, M., 1987. Comparaison des distributions de l'iridium observées à la limite Crétacé–Tertiaire dans divers sites européens. Mém. Soc. Géol. Fr., 150: 95–103.

Romein, A.J.T. and Smit J., 1981. The Cretaceous/Tertiary boundary: Calcareous nannofossils and stable isotopes. Proc. K. Ned. Akad. Wet., 84: 295–314.

Rosenkrantz, A., 1937. Bemaerkninger om det Ostsjaellandske Daniens stratigrafi og tektonik. Medd. Dan. Geol. Foren., 9: 199–212.

Rosenkrantz, A., 1966. Die Senon/Dan-Grenze in Dänemark. Ber. Dtsch. Ges. Geol. Wiss., A, Geol. Paläontol., 11: 721–727.

Schmitz, B., 1987. Barium, equatorial high productivity, and the northward wandering of the Indian continent. Paleoceanography, 2: 63–77.

Schmitz, B., 1988. Origin of microlayering in worldwide distributed Ir-rich marine Cretaceous/Tertiary boundary clays. Geology, 16: 1068–1072.

Schmitz, B., 1990a. Reply on Comment on "Origin of microlayering in worldwide distributed Ir-rich marine Cretaceous/Tertiary boundary clays". Geology, 18: 89–92.

Schmitz, B., 1990b. Reply on Comment on "Origin of microlayering in worldwide distributed Ir-rich marine Cretaceous/Tertiary boundary clays". Geology, 18: 93–94.

Schmitz, B., Asaro, F., Michel, H.V., Thierstein, H.R. and Huber, B.T., 1991. Element stratigraphy across the Cretaceous/Tertiary boundary in Hole 738C. In: Proc. ODP Sci. Res., 119: 719–730.

Sliter, W.V., 1972. Cretaceous foraminifera depth habitats and their origin. Nature, 239: 514–515.

Smit, J., 1990. Meteorite impact, extinctions, and the Cretaceous/Tertiary boundary. Geol. Mijnbouw, 69: 187–204.

Smit, J. and Ten Kate, W.G.H.Z., 1982. Trace element patterns at the Cretaceous–Tertiary boundary-consequences of a large impact. Cretaceous Res., 3: 307–332.

Stenestad, E., 1971. Træk av det danske bassins udvikling i Øvre Kridt. Dan. Geol. Fören. Årsskr., 1971: 63–69.

Stott, L.D. and Kennett, J.P., 1989. New constraints on early Tertiary paleoproductivity from carbon isotopes in foraminifera. Nature, 342: 526–529.

Surlyk, F., 1979. Guide to Stevns Klint. In: T. Birkelund and R.G. Bromley (Editors), Cretaceous–Tertiary boundary events, I. The Maastrichtian and Danian of Denmark. Univ. Copenhagen, pp. 164–170.

Sweet, A.R., Braman, D.R. and Lerbekmo, J.F., 1990. Palynofloral response to K/T boundary events; A transitory interruption within a dynamic system. Geol. Soc. Am. Spec. Pap., 247: 457–469.

Thierstein, H.R., Asaro, F., Ehrmann, W.U., Huber, B., Michel, H.V., Sakai, H. and Schmitz, B., 1991. The Cretaceous/Tertiary boundary at Site 738, southern Kerguelen Plateau. In: Proc. ODP Sci. Res., 119: 849–861.

Vincent, E., Killingley, J.S. and Berger, W.H., 1981. Stable isotope composition of benthic foraminifera from the equatorial Pacific. Nature, 289: 639–643.

Wu, G. and Berger, W.H., 1989. Planktonic foraminifera: Differential dissolution and the Quaternary stable isotope record in the west Equatorial Pacific. Paleoceanography, 4: 181–198.

Wu, G., Herguera, J.C. and Berger, W.H., 1990. Differential dissolution modification of late Pleistocene oxygen isotope records in the western Equatorial Pacific. Paleoceanography, 5: 581–594.

Zachos, J.C. and Arthur, M.A., 1986. Paleoceanography of the Cretaceous/Tertiary boundary event: Inferences from stable isotopic and other data. Paleoceanography, 1: 5–26.

Zachos, J.C., Arthur, M.A. and Dean, W.E., 1989. Geochemical evidence for suppression of pelagic marine productivity at the Cretaceous/Tertiary boundary. Nature, 337: 61–64.

Zahnle, K. and Grinspoon, D., 1990. Comet dust as a source of amino acids at the Cretaceous/Tertiary boundary. Nature, 348: 157–160.

Zhao, M. and Bada, J.L., 1989. Extraterrestrial amino acids in Cretaceous/Tertiary boundary sediments at Stevns Klint, Denmark. Nature, 339: 463–465.